TURUN YLIOPISTON JULKAISUJA
ANNALES UNIVERSITATIS TURKUENSIS

SARJA - SER. A I OSA - TOM. 457

ASTRONOMICA - CHEMICA - PHYSICA - MATHEMATICA

BIOPHYSICAL MODELLING OF PHOTOSYNTHETIC ELECTRON TRANSFER AND PRACTICAL APPLICATIONS TO CYANOBACTERIA

by

Susanne Rantamäki

TURUN YLIOPISTO
UNIVERSITY OF TURKU
Turku 2013

From the Laboratory of Molecular Plant Biology
Department of Biochemistry and Food Chemistry
University of Turku
FI-20014 Turku, Finland

Supervised by
Dr. Esa Tyystjärvi
Dr. Taina Tyystjärvi

Laboratory of Molecular Plant Biology
Department of Biochemistry and Food Chemistry
University of Turku, FI-20014 Turku, Finland

Reviewed by

Professor Eero Nikinmaa
Department of Forest Science
University of Helsinki
FI-00014 Helsinki, Finland

and

Dr. Fikret Mamedov
Department of Chemistry
Uppsala University
Uppsala, 75120 Sweden

Opponent

Dr. Ladislav Nedbal
Global Change Research Centre
Academy of Sciences
Drasov, Czech Republic

ISBN 978-951-29-5295-3 (PRINT)
ISBN 978-951-29-5296-0 (PDF)
ISSN 0082-7002
Painosalama Oy – Turku, Finland 2013

LIST OF ORIGINAL PUBLICATIONS

This thesis is based on following articles, which are referred to by their Roman numerals in the text.

I. **Rantamäki S., Meriluoto J., Spoof L., Puputti E.-M., Tyystjärvi E.** (2013) Cyanobacteria tolerate high iron concentrations in anaerobic conditions, confirming their possible importance in Archaean oceans. Manuscript.

II. **Tyystjärvi E., Rantamäki S., Tyystjärvi J.** (2009) Connectivity of Photosystem II is the physical basis of retrapping in photosynthetic thermoluminescence. Biophysical Journal 96, 3735-3743

III. **Rantamäki S., Tyystjärvi E.** (2011) Analysis of $S_2Q_A^-$ charge recombination with the Arrhenius, Eyring and Marcus theories. Journal of Photochemistry and Photobiology B: Biology 104, 292-300.

IV. **Pollari M., Rantamäki S., Huokko T., Kårlund-Marttila A., Virjamo V., Tyystjärvi E., Tyystjärvi T.** (2011) Effects of Deficiency and Overdose of Group 2 Sigma Factors in Triple Inactivation Strains of *Synechocystis* sp. Strain PCC 6803. Journal of Bacteriology 193, 265–273.

V. **Rantamäki S., Tyystjärvi T.** (2013) Light acclimation of triple inactivation strain of group 2 sigma factors in *Synechocystis* sp.strain PCC 6803. Proceedings of the 15th International Congress on Photosynthesis, Beijing, China (in press).

ABBREVIATIONS

A_{730}	absorbance at 730 nm
APC	allophycocyanin
BA	billions of years ago
BIF	banded iron formation
BL	blue light
BG-11	growth medium for *Synechocystis* sp. PCC 6803
Chl	chlorophyll
^{3}Chl	triplet chlorophyll
CO_2	carbon dioxide
CS	control strain, glucose tolerant strain of *Synechocystis* sp. PCC 6803
Cyt b_6f	cytochrome b_6f complex
DCMU	3-(3,4-dichlorophenyl)-1,1-dimethyl urea
DLE	delayed light emission
E_a	activation energy
Fd	ferredoxin
Fe^{2+}	ferrous iron
Fe^{3+}	ferric iron
Fe-S	iron-sulfer center
F_M	maximum fluorescence
FNR	ferredoxin-$NADP^+$ reductase
FRP	fluorescence recovery protein
F_V	variable fluorescence
F_0	minimum fluorescence
ΔG_a	activation free energy
GL	standard growth light
h	Planck's constant
ΔH_a	activation enthalpy
ΔS_a	activation entropy
IsiA	iron-deficiency-induced IsiA protein, CP43'
J	a constant describing energetic connectivity of PSII

k_b	Boltzmann's constant
LHC	light-harvesting complex
NPQ	non photochemical quenching
OCP	orange carotenoid protein
OEC	oxygen evolving complex
PAM	pulse amplitude modulation
PC	plastocyanin
PCC	Pasteur Culture Collection
Pheo	pheophytins
PPFD	photosynthetic photon flux density
PQ	plastoquinone pool
PSI	photosystem I
PSII	photosystem II
P_{680}	reaction center chlorophyll of PSII
P_{700}	reaction center chlorophyll of PSI
Q_A	primary quinone acceptor of PSII
Q_B	secondary quinone acceptor of PSII
S_0, S_1, S_2, S_3, S_4	S-states of OEC
s_0	pre-exponential factor of Arrhenius equation
TL	thermoluminescence
UHCC	University of Helsinki Culture Collection
Y_Z	tyrosine residue 161 of the D1 protein
Z8	growth medium for *Nodularia* and *Microcystis*

TABLE OF CONTENTS

ABSTRACT

Cyanobacteria have a similar photosynthesis as plants. Despite of their tiny size, cyanobacteria have had a revolutionary effect on Earth's evolution and they are still responsible for at least one third of global primary production. I have studied the possible role of cyanobacteria in the oxygenation of the atmosphere and the oceans during the Archaean time. The results showed that cyanobacteria are able to live in anaerobic conditions in the presence of high concentrations of ferrous iron. These conditions mimic those in Archaean oceans. Furthermore, oxygen produced during photosynthesis caused precipitation of iron. The results suggest that cyanobacteria may have caused the massive precipitation of iron that led to the build-up of banded iron formations during Archaean era. The results also show that microcystins or nodularins do not play important role in iron metabolism.

In the second part of the study, I modeled thermoluminesence and chlorophyll *a* fluorescence. The focus was on the reaction in which the charge separated state $S_2Q_A^-$ recombines, forming the ground state S_1Q_A. $S_2Q_A^-$ recombination is associated with a decrease in chlorophyll *a* fluorescence yield and with the Q band of thermoluminescence. The results showed that energy transfer between photosystem II centers widens the Q band and shifts the peak to a lower temperature. Comparison of thermoluminescence data with measurements of decay of chlorophyll *a* fluorescence yield showed that a common model can be applied to both phenomena. For the first time, the Marcus theory of electron transfer reactions was applied to photosynthetic thermoluminescence.

The group 2 σ factor triple inactivation strains ΔsigBCD, ΔsigBCE, ΔsigBDE and ΔsigCDE of *Synechocystis* sp. PCC 6803 were analyzed with the biophysical methods. The biophysical methods revealed differences in light acclimation in these strains. All triple inactivation strains had a higher photosystem II peak in 77 K fluorescence spectra than the control strain, and the ΔsigBCE strain was found to be locked to state 1. Absorption spectra revealed that ΔsigCDE (with SigB as the only group 2 σ factor) has more carotenoids than the control strain and in photoinhibition experiments the ΔsigCDE strain behaved like the control strain while all other triple inactivation strains were more sensitive to light than the control strain. *Synechocystis* cells lacking SigB and SigD simultaneously were unable to use high light as efficiently as the control strain. These data show that SigB factor is important for acclimation to high light.

1. INTRODUCTION

1.1. Cyanobacteria

1.1.1. Ancient Earth and first cyanobacteria

The Earth is over 4.5 billion of years old (Nisbet and Sleep, 2001), and conditions in ancient Earth were quite different than nowadays. There was no oxygen in the atmosphere and the carbon dioxide content was higher. Temperature has been fluctuating from warm (70°C) to cold (worldwide ice ages) during different periods in Earth's early history. The environment in ancient oceans was rich in different metals such as iron and manganese. The first life forms were prokaryotes and the first evidence for biological carbon fixation are fossil stromatolites which are dated as 3.4 billion of years old (Schidlowski, 1988). Most probably, photosynthesis evolved via anoxygenic forms resembling current photosynthetic anoxygenic bacteria. Anoxygenic photosynthetic organism have either a reaction center complex resembling photosystem I (PSI) or one resembling photosystem II (PSII) (Bryant and Frigaard, 2006).

Oxygenic photosynthesis, employing both PSII and PSI, evolved in cyanobacteria. Oxygen, a side product of oxygenic photosynthesis, caused huge changes in the ancient environment. In oceans, oxygen reacted fast with metals, forming both soluble and insoluble compounds. Geochemical evidence suggests that oxygen appeared in Earth's atmosphere 2.45 billion years ago (BA) (Bekker, et al., 2004; Claire, et al., 2006). However, the oxygen content of oceans may have started to rise long before oxygen escaped to the atmosphere, and the actual timing of the emergence of cyanobacteria is still unclear. The oldest microfossils tentatively identified as cyanobacteria are 3.5 billion of years old (Schopf and Packer, 1987; Schopf, 1993) but they might be fossils of filamentous non-oxygen-evolving phototrophs (Pierson, 1994), sulfur metabolizing organisms (Bontognali, et al., 2012) or even abiogenic structures (Brasier, et al., 2002).

Banded iron formations (BIF) are iron rich stones which were formed in oceans mainly during the Archaean and early Proterozoan era (2.5-1.8 BA) but the oldest known BIF is dated as 3.8 BA (Rosing, et al., 1996). Most of the mineable iron of the Earth's crust is in these stones. BIFs are striped by two layers, an iron rich reddish layer and an iron poor gray or dark layer (James, 1954). The thickness of these layers is from a few millimeters to a few centimeters. The origin of these formations is under debate and there are several different hypotheses. The BIFs could be born when oxygen produced by

photosynthetic cyanobacteria oxidized the soluble ferrous iron (Fe^{2+}) to ferric iron (Fe^{3+}) which then precipitated, or they may have been formed by anoxygenic phototrophic bacteria (Widdel, et al., 1993). It could be speculated that the layered structure of the BIFs results from the toxicity of oxygen to cyanobacteria. In this case, precipitation of iron would have ended due to the toxicity of free oxygen, and started again only after mixing of the ocean water and re-establishment of a cyanobacterial population. However, the long time of BIF formation speaks against this interpretation, as cyanobacteria would be expected to have evolved protective mechanisms. Also ultraviolet light (Cairnssmith, 1978) and hydrothermal plumes (Isley and Abbott, 1999) have been proposed to be behind oxidation of Fe^{2+}.

1.1.2. Current cyanobacteria

According to the endosymbiosis theory, cyanobacteria are the progenitors of primary plastids including the chloroplasts of higher plants, green and red algae and the Glaucocystophyta (Keeling, 2004; Rodriguez-Ezpeleta, et al., 2005). Even after evolution of photosynthetic eukaryotes, cyanobacteria remain as extremely important producers in ecosystems. Cyanobacteria are responsible for at least one third of the net primary production on the Earth (Field, et al., 1998; Bryant, 2003).

Cyanobacteria are gram negative eubacteria, and some species are unicellular while other species form filaments. Filaments may contain specialized cells like akinetes or heterocysts. In addition to carbon fixation, some cyanobacteria are able to fix nitrogen. This biological nitrogen fixation is catalyzed by nitrogenases which are sensitive to O_2 (Fay, 1992). For that reason, nitrogen fixation and O_2 evolution are either temporally or spatially separated. Some filamentous cyanobacteria, like *Nodularia*, have specialized nitrogen fixing cells called heterocysts that have thick cell walls to prevent oxygen diffusion to the cell and that do not have PSII (Fay, 1992). Cyanobacteria which use temporal separation mechanism are photosynthetically active in the light and fix nitrogen in darkness (Misra and Tuli, 2000).

In the public eye, cyanobacteria are mostly known for their ability to produce cyanotoxins. In particular, cyanobacteria produce cyclic heptapeptides (microcystins) or pentapeptides (nodularins). These toxins inhibit protein phosphatases, which causes the toxicity to other organisms (Jaiswal, et al., 2008). The production of toxins is an ancient trait in cyanobacteria (Rantala, et al., 2004) but many cyanobacteria species have lost their ability to produce toxins during evolution. The roles of cyanotoxins are still unclear, but there are some hypotheses. They might have allelopathic effects on some algae and against herbivores (Babica, et al., 2006). The toxins resemble chemically bacterial siderophores and can form complexes with iron (Utkilen and Gjolme, 1995)

and other metals (Humble, et al., 1997). Iron may also induce microcystin production (Utkilen and Gjolme, 1995). These data may suggest that the toxins may have a role in iron metabolism. It has also been proposed that the toxins function as intraspecific signaling molecules (Dittmann, et al., 2001).

1.2. Photosynthesis and light harvesting in plants and cyanobacteria

Photosynthesis can be separated to light reactions and the Calvin-Benson cycle. In light reactions, light energy is converted to chemical energy in the form of ATP and NADPH, and oxygen is released as a side product. In the Calvin-Benson cycle, the energy of ATP and NADPH is then used to assimilate carbon dioxide to triose phosphates (Bräutigam and Weber, 2011).

Photosynthetic light reactions occur in the thylakoid membranes. The major multisubunit protein-pigment complexes in thylakoid membranes are PSII, the cytochrome b_6f complex, PSI and the ATP synthase. The structure of PSII at 1.9 Å resolution (Umena, et al., 2011), and that of PSI at 2.5 Å (Jordan, et al., 2001) have been resolved. The PSII core proteins are very similar in plants and cyanobacteria, but the light harvesting antenna systems are different.

In plants, the membrane intrinsic chlorophyll-binding light harvesting complex (LHC) proteins function as the main antenna complexes of PSII and PSI. LHCII is the major antenna complex of PSII, and the reaction center of PSII and LHCII form the PSII-LHCII supercomplex (Boekema, et al., 2000). The LHCII is a trimer formed of Lhcb1, Lhcb2 and Lhcb3 proteins (Jansson, 1994). There are two or three LHCII trimers per one PSII reaction center. In addition to LHCII, antenna of PSII contains so called small Chl *a/b* proteins (Ganeteg, et al., 2004). PSI has its own light harvesting complex called LCHI which consists of proteins having amino acid sequences highly similar to the proteins of LHCII (Boekema, et al., 2001). LHCI is composed of four Lhca proteins (Lhca1–Lhca4) and there are four LHCI heterodimers per one PSI (Wientjes, et al., 2011). Cyanobacteria have neither LHCI nor LHCII.

Cyanobacteria have a distinct light harvesting phycobilisome antenna that can be associated with PSII and PSI (Adir, 2005). Phycobilisomes are composed of water-soluble protein subunits carrying covalently attached phycobilin pigments (Mullineaux, 2008). The phycobilisomes do not bind Chl. Large phycobilisomes consist of more than 100 polypeptides and structurally two different parts, the core and the rods, can be distinguished (Fig. 1) (Grossman, et al., 1993). In *Synechocystis*, the phycobilisome antenna consists of six phycocyanin rods; and every rod consists of three hexameric disks on top of each other (Fig. 1). The absorption maximum of the phycocyanin

containing rods is 620 nm, and the fluorescence maximum is from 640 nm to 650 nm. The core of the phycobilisome consists of three allophycocyanin (APC) cylinders, each of them consisting of four trimeric disks. The two cylinders closest to the membrane emit at 680 nm. The cylinder consists of two 3αβAPC disks which emit at 660 nm (APC_{660}) and two other disks where the α- or β subunit is replaced by ApcD, ApcF or ApcE (MacColl, 1998; Arteni, et al., 2009). This replacement of one of the α or β subunits changes the emitted wavelength. The third cylinder consists of four 3αβAPCs and thus emits at 660 nm. All pigment proteins in the phycobilisome antenna are bound to each other by several different types of linker proteins, and the phycobilisome antenna is attached to the membrane by several weak charge-charge interactions (Mullineaux, 2008). The phycobilisome antenna is flexible and is able to diffuse on the thylakoid membrane, and also between PSII and PSI (Mullineaux, et al., 1997; Sarcina, et al., 2001). It has been proposed that the phycobilisome antenna has a low specify for binding to different membrane components (Mullineaux, 2008). This enables fast rearrangement in changing light conditions. Phycobilisomes are efficient antenna systems, and they are able to funnel over 90 % of captured light energy to PSII or PSI via APC_{680} (Grossman, et al., 1993; Dong, et al., 2009).

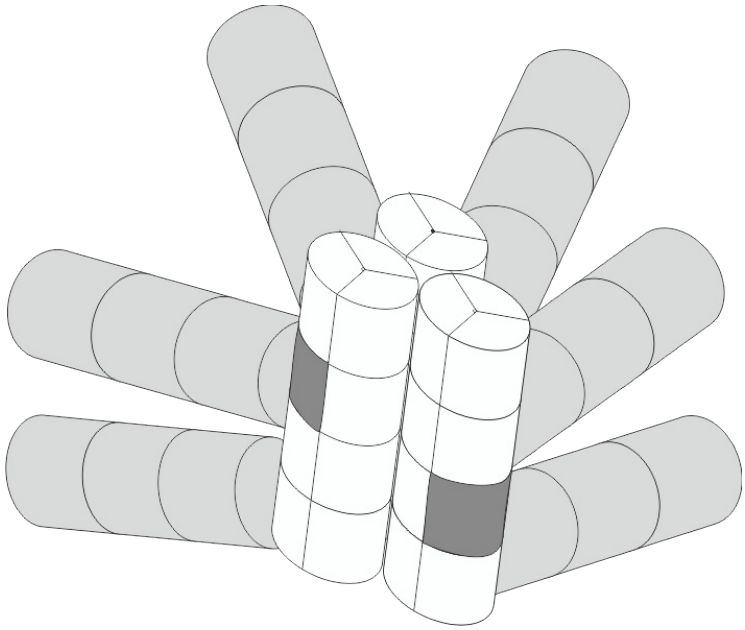

Figure 1. Structure of phycobilisome antenna of *Synechocystis*. The light grey cylinders are the rods and white cylinders form the core. Dark grey parts in the core are the subunits APC_{680}. Modified from Tian, et al. (2012).

1.3. Analyses of photosystem II

1.3.1. Electron transfer in PSII

PSII is a thylakoid embedded pigment-protein complex composed of more than 20 subunits with a molecular mass of 350 kDa (Ferreira, et al., 2004). In addition to polypeptides, the PSII monomer contains 35 Chl, two pheophytins, 11 β-carotenes, over 20 lipids, two plastoquinones, two haem irons, one nonhaem iron, four manganese atoms, three or four calcium atoms, three Cl^- ions and one bicarbonate ion (Umena, et al., 2011).

PSII transfers electrons across the thylakoid membrane from water to the plastoquinone pool, and oxygen is released as a side product. Water splitting occurs in the oxygen evolving complex of PSII. In forward electron transfer reactions of PSII, a photon excites an antenna pigment molecule and the exited state moves to the reaction center Chl P_{680} (Fig. 2). An exited primary electron donor P_{680}^* reduces a pheophytin, and the pheophytin reduces a plastoquinone molecule Q_A. Q_A^- then reduces another plastoquinone molecule Q_B. After double reduction and protonation the reduced plastoquinone molecule is replaced with an oxidized one from the plastoquinone pool.

The hole in the primary donor is filled by an electron from the oxygen-evolving manganese complex via Y_Z that is a tyrosine residue 161 of the D1 protein (Debus, et al., 1988). The consecutive oxidations of the OEC are described as an S-state cycle containing five different oxidation states S_0-S_4 (Kok, et al., 1970).

After formation of the state $S_2Q_A^-$ or $S_2Q_AQ_B^-$, an electron has a certain low probability to move backwards from Q_A^- or Q_B^- and recombine with the S_2 state of the oxygen evolving complex, producing S_1Q_A or $S_1Q_AQ_B$, respectively. A similar charge recombination may occur between S_3 and Q_A^- or Q_B^-. The charge pairs produced by electron transfer reactions of PSII, e.g. $P_{680}^+ Q_A^-$, are stabilized by loss of free energy. Respectively, the recombination of a charge pair requires input of activation energy. If P_{680}^* is an intermediate of a recombination reaction, then the activation energy equals the energy lost in stabilization. For this reason, analysis of the recombination reactions gives important information about forward electron transfer reactions as well.

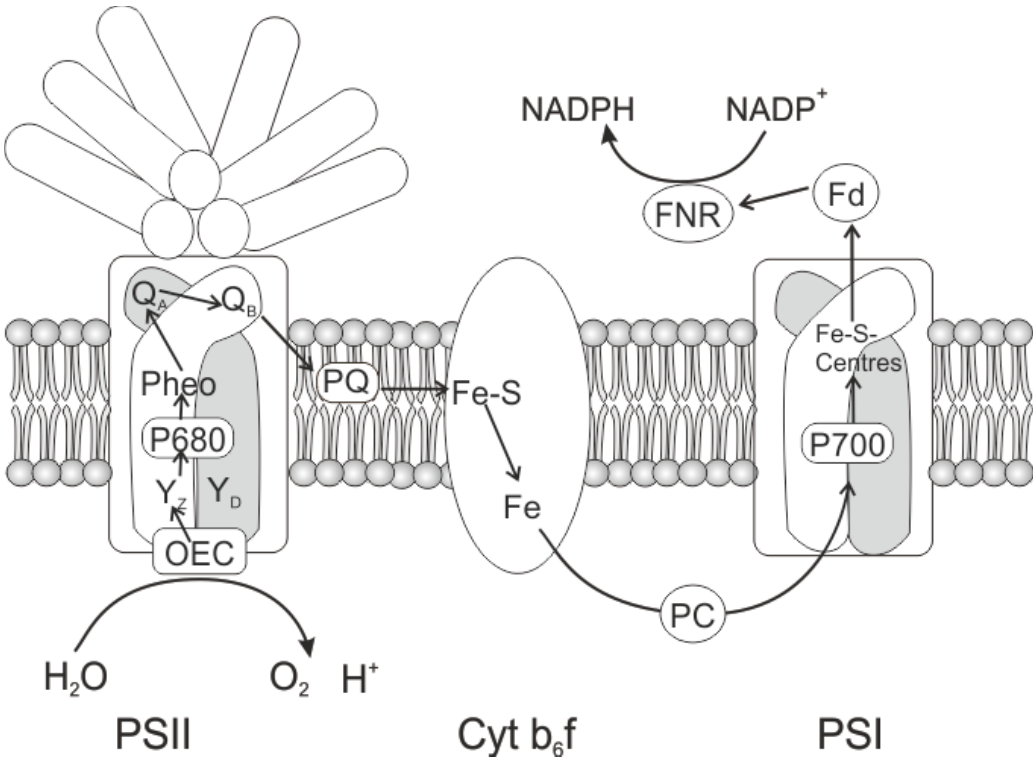

Figure 2. The linear photosynthetic electron transfer chain in cyanobacteria. Light excites P_{680} and an electron is transferred to pheophytin (Pheo). P_{680} gets an electron via a tyrosin residue (Y_Z) from the oxygen evolving complex (OEC) which pulls electrons out of water. From Phe electron moves to plastoquinone Q_A and further to a second plastoquinone Q_B. Q_B receives two electrons and dissociates from PSII to the plastoquinone pool, and passes electrons to the cytochrome b_6f complex (Cyt b_6f) where an electron moves first to an iron-sulfur center (Fe-S) then to a heme iron (Fe) and finally to plastocyanin (PC). The Q cycle (not shown) enhances proton pumping by Cyt b_6f). Light excites P_{700} and an electron moves from P_{700} via iron-sulfur-centers (Fe-S-centers) to ferredoxin (Fd) and finally to ferredoxin-$NADP^+$ reductase (FNR). PC carries an electron from the Cyt b_6f complex to $P_{700}{}^+$.

1.3.2. Oxygen evolution

The function of PSII can be measured by oxygen evolution. Oxygen measurements with an artificial quinone as an electron acceptor are used to measure the function of PSII alone. Artificial electron acceptors can be used with isolated thylakoids, and *in vivo* with cyanobacteria and many microalgae (Renger and Hanssum, 2009). In the presence of an artificial electron acceptor of PSII, the rate of oxygen evolution obtained in saturating light is proportional to the amount of active PSII reaction centers in the sample, and measurements in limiting light monitor the function of PSII in growth conditions.

The rate of O_2 evolution measured with CO_2 as the electron acceptor is affected both light and dark reactions of photosynthesis. If photosynthesis is measured in high light, the carbon cycle limits the rate of oxygen evolution, whereas the light reactions limit in low light.

1.3.3. Fluorescence of photosynthetic pigments

Chl and phycobilins emit fluorescence in the red to far-red range. The emission spectrum of a photosynthetic organism depends strongly on temperature and the spectra are often measured at 77 K. The 77 K spectra show two peaks of PSII (at 685 and 695 nm) and one peak of PSI (at 725 nm, cyanobacteria). If the emission spectrum is measured from cyanobacteria by using orange exciting light, also a phycobilisome peak is present (at 640–650 nm). If the exciting light is blue, the phycobilisome peak does not appear because blue light excites only Chl *a* and not the phycobilins. Emission spectra can be used to measure the ratios of the photosynthetic complexes.

Chl fluorescence can be used to monitor the function of the photosynthetic electron transfer reactions. Most applications of Chl *a* fluorescence are based on the fact that the yield of Chl *a* fluorescence depends on the reduction state of Q_A. Maximum fluorescence (F_M) is detected when all Q_A are reduced, i.e. the reaction centers are closed. The minimum level (F_0) is detected in the opposite situation when all reaction centers are open (all Q_A oxidized). Variable fluorescence (F_V), in turn, is fluorescence detected above F_0, and the quantum yield of variable fluorescence is roughly proportional to the ratio $Q_A^-/(Q_A + Q_A^-)$. With a pulse amplitude modulation (PAM) fluorometer, changes in the yield of Chl *a* fluorescence can be measured in the presence of background light. PAM fluorometry can be used for measurements of non-photochemical quenching and state transitions. Chl *a* fluorescence can also be used to measure back electron transfer reactions of PSII, as the recombination reaction $S_2Q_A^- \rightarrow S_1Q_A$ causes a decrease in fluorescence. This recombination reaction is the same that causes the Q band of thermoluminescence (TL) and thus it should be possible to analyze the behavior of fluorescence and TL with a common model.

Connectivity is a phenomenon in which excitation energy can migrate from a closed reaction center to an open reaction center. This connectivity is the reason for the sigmoidal shape of the fluorescence induction curve in the presence of DCMU (Lavergne and Trissl, 1995). The effect of connectivity is also expected to affect TL measurements.

1.3.4. Thermoluminescence

Photosynthetic TL was found by Arnold and Sherwood (1957) and it can be described by a TL model for solid materials (Randall and Wilkins, 1945). Photosynthetic TL curves

originate from PSII. In TL measurements, a flash of light is given at low temperature to cause a charge separation, and the sample is then heated at a constant rate, which leads to a peak of luminescence at a temperature that depends on the free energy of activation of the recombination reaction.

Many of TL peaks are found at very low temperatures. Photosynthetic energy transfer reactions are not involved in the low temperature peaks (Noguchi, et al., 1993), and they rise from energy stored in Chl *a* and Chl *b* at -253°C, -223°C and -203°C. The Z peak at -160°C originates most probably from recombination of the pair Chl^+ Chl^- (Sonoike, et al., 1991). The Z_V peak occurs from -80°C to -33°C; the position of peak depends on the temperature at which the exciting flash was given. This peak originates presumably from recombination of P_{680}^+ and Q_A^- (Chapman, et al., 1991). A peak at -15°C (A band) originates from the recombination of $Y_Z^+Q_A^-$. If a thylakoid sample is treated with Tris to remove manganese, an A_T peak originates from the recombination of the $His^+Q_A^-$ pair (Koike, et al., 1986).

Two important peaks occur between 0°C and 50°C. When DCMU is added it binds to the Q_B pocket of PSII and prevents electron transfer from Q_A^- to Q_B. The TL peak at +5°C to +20°C observed in the presence of DCMU is called as the Q band. The Q band originates from recombination reactions of $S_2Q_A^-$ and $S_3Q_A^-$ (Rutherford, et al., 1982; Demeter, et al., 1984; Demeter and Vass, 1984). The B band, approximately at +35°C, can be divided to two different peaks. The B1 band originates from the reaction $S_2Q_AQ_B^- \rightarrow S_1Q_AQ_B$ and the B2 band from the reaction $S_3Q_AQ_B^- \rightarrow S_2Q_AQ_B$ (Rutherford, et al., 1982; Demeter and Vass, 1984). However, these two peaks can be seen separately only in low pH 4.5–6.0 and in neutral conditions they are identical (Inoue, 1981).

The C band at +50°C is luminescence from the recombination of Tyrosine $D^+Q_A^-$ (Rutherford, et al., 1982; Demeter, et al., 1984). Addition of DCMU makes the intensity of the C band higher. When TL is measured from intact samples (like chloroplasts or leaves) the recombination of the pair $S_{2(3)}Q_B$ produces the after glow peak (AG) at +40°C to +50°C. The AG band can be initiated by illumination with far red light at room temperature.

The peaks observed at still higher temperature are not related to PSII electron transfer. Oxidative chemiluminescence of protein binding pigments (Vass, et al., 1989; Hideg and Vass, 1992) produces a peak between +47°C and +70°C, and peroxidation of lipids is responsible of peaks around +125°C (Ducruet and Vavilin, 1999).

The Q and B bands are the most studied bands. The Q band deviates from an ideal first-order TL band, which causes a particular problem in using the Q band for analyzing the $S_2Q_A^-$ recombination. Different models have been put forward to explain the deviation (Tyystjärvi and Vass, 2004). Rappaport, et al. (2002, 2005) presented a model where the

recombination reaction occurs via three different reaction routes and only one of these routes produces luminescence. This model explains why the recombination of the $S_2Q_A^-$ pair seems to occur more slowly when studied with TL than when fluorescence is used to measure the reaction.

1.3.5. Delayed light emission

Delayed light emission (DLE) is luminescence measured as function of time at constant temperature. Photosynthetic DLE was found by Strehler and Arnold (1951). Photosynthetic luminescence mainly originates from PSII, and PSI only emits very short-lived DLE. The time scale of DLE is from nanoseconds to minutes. The fast (µs-ms) components originate from recombination of $Z^+P_{680}Q_A^-$ and the slow ones (from ten seconds to minutes) from $S_2Q_A^-$ and $S_3Q_A^-$ recombination (Rutherford and Inoue, 1984). The intensity of DLE relative to the luminescence intensity at zero time after a single turnover flash depends on three parameters i) the amount of PSII ii) the rate of the recombination reaction and iii) how big proportion of the recombination reactions produces luminescence.

1.3.6. Arrhenius, Eyring and Marcus theories of the reaction rate constant

The rate of a reaction is determined by the concentrations (chemical activities) of the reactants and by a reaction-specific factor called the rate constant. The structure of the rate constant has been a topic of theoretical analysis in chemistry from the time of Svante Arrhenius, who first explained why temperature speeds up chemical reactions and who introduced the term activation energy, E_a. E_a is the energy that has to be obtained from the environment before a chemical reaction can occur, and the reaction rate depends on E_a. Increase in temperature increases the movement of molecules and thereby also their energy. The Arrhenius equation is

$$k = s_0 e^{\frac{-E_a}{k_b T}} \tag{1}$$

where s_0 is a temperature independent pre-exponential constant and k_b is the Boltzmann constant. k_b is a constant which tells the how much energy the reactants gain when temperature raises by one Kelvin. The exponential component of the Arrhenius equation describes the proportion of molecules whose energy is larger than E_a according to the Maxwell-Boltzmann distribution.

The further developed Eyring theory (Glasstone, et al., 1941) takes into account the transition state theory. In the Eyring theory, the temperature independent E_a was replaced by activation free energy, also called the Gibbs energy (ΔG_a), which depends on temperature according to the equation

$$\Delta G_a = \Delta H_a - T\Delta S_a \tag{2}$$

where ΔH_a is activation enthalpy and ΔS_a is activation entropy. Another difference between Arrhenius and Eyring equations is in the pre-exponential factor, as the temperature independent constant s_0 of the Arrhenius equation is replaced by a universal temperature depended constant value A in the Eyring theory. For monomolecular reactions A is

$$A = \frac{k_b T}{h} \tag{3}$$

where h is Planck's constant. In addition, the Eyring theory applies transmission factors that take into account that reactions can occur only if the reactants meet each other. In analysis of TL it was assumed that the transmission factor is unity. The Eyring equation for the reaction rate constant is

$$k = \frac{k_b T}{h} e^{\frac{T\Delta Sa - \Delta Ha}{k_b T}} \tag{4}$$

The fact that in the Eyring model both the pre-exponential and exponential factor depend on temperature, causes problems in extracting the thermodynamic parameters from kinetic data. For example, the data of Paper II could equally well be fitted by using a positive ΔS_a and somewhat higher ΔH_a than reported. However, we chose to use a negative ΔS_a on the basis of literature. The Marcus theory has a similar property.

While both Arrhenius and Eyring theories deal primarily with molecular reactions of gases, the Marcus theory is developed specifically to explain electron transfer reactions. Also in the Marcus theory the equation can be divided to a pre-exponential and an exponential factor. The equation for the rate constant is

$$k = \frac{2\pi}{\hbar} \left| H_{AB} \right|^2 \frac{1}{\sqrt{4\pi\lambda k_b T}} e^{\left(-\frac{(\lambda + \Delta G^0)^2}{4\lambda k_b T}\right)} \tag{5}$$

where ħ is the reduced Planck's constant (ħ = h/2π), $|H_{AB}|$ quantifies the electronic coupling between the initial and final states, l is the solvent reorganization energy, and ΔG° is the standard free energy change of the reaction. The Marcus theory explains the nature of the activation energy with the balance between the free energy change of the reaction and the energy required to reorganize solvent molecules during the reaction.

1.4. Acclimation of photosynthesis

1.4.1. Photoinhibition

Photoinhibition is a phenomenon in which light causes decrease of photosynthetic activity. The main target of photoinhibition is PSII. There are several different hypotheses on the mechanism of photoinhibition. The earlier main hypotheses were the acceptor-side, low-light and donor-side mechanisms. In the acceptor side hypothesis, it is assumed that under excess light, over-reduced plastoquinone pool slows down electron transfer from Q_A^- to Q_B, which finally leads to double reduction and dissociation of Q_A (Vass, et al., 1992). Consequentially, the lifetime of the primary radical pair is prolonged and the probability of triplet Chl (^{3}Chl) production is increased. ^{3}Chl, in turn, may promote production of singlet oxygen. The low-light hypothesis has been created to explain why photoinhibition occurs in dim light. Under very low light the quantum yield of the recombination reactions between the S_2 and S_3 states of OEC and the quinone acceptors of PSII increases (Keren, et al., 1995) leading to a higher probability of ^{3}Chl and singlet oxygen production. In the donor-side hypothesis, electron donation from the OEC is disturbed and the long lived P_{680}^+ oxidizes PSII reaction center components (Callahan and Cheniae, 1985; Jegerschöld and Styring, 1996). Also donor-side photoinhibition can produce reactive oxygen species (Hideg, et al., 1994). In the manganese hypothesis, light inactivates the OEC by removing a Mn ion from the Mn-cluster. After this, light is absorbed by Chl and damage is caused by P_{680}^+ or singlet oxygen (Hakala, et al., 2005).

As recombination reactions have been suggested to be important in photoinhibition, better understanding of the recombination reactions might open up pathways for biotechnology that could relieve the stress caused by reactive oxygen species to plants and cyanobacteria

1.4.2. State transitions

State transitions balance the energy distribution between PSII and PSI, optimizing the use of light energy (Bonaventura and Myers, 1969; Murata, 1969). In state 1, light

energy is mainly transferred to PSII and in state 2 energy capture by PSI is favored (Bonaventura and Myers, 1969; Murata, 1969). Light harvesting complexes are different in cyanobacteria and in plants, and the mechanism of state transitions differs between cyanobacteria and plants. In plants, phosphorylation of LHCII proteins and thylakoid rearrangements are involved in state transitions (Bennett, et al., 1980; Lemeille and Rochaix, 2010). In cyanobacteria, rearrangement of the phycobilisome antenna between PSII and PSI has a central role (Mullineaux, 1992; van Thor, et al., 1998). In higher plants, state transitions are regulated by the redox state of the plastoquinone pool (PQ) but in cyanobacteria, the details of the regulation are not known. State transitions are physiologically important for growth in dim light (Murata, 1969; Emlyn-Jones, et al., 1999).

State transitions can be detected by fluorescence measurements. In cyanobacterial state transition, blue light induces a transition from state 2 to state 1 and a rise of the fluorescence maximum (F_M). Orange light, in turn, excites phycobilisomes which are connected to PSII in state 1, and this leads a state 1 to state 2 transition. The intensity and rate of state transitions decreases at lower temperatures. State transitions can be measured either at a physiological temperature by following the F_M level with a PAM fluorometer, or by measuring the ratio of PSII and PSI emission peaks at 77 K.

1.4.3. Non-photochemical quenching

Non-photochemical quenching (NPQ) protects plants and cyanobacteria from excessive light by removing the excess energy as heat. In plants, the PsbS protein and conversion of violaxanthin to zeaxanthin are required for NPQ (Li, et al., 2000; Niyogi, et al., 2005). Cyanobacteria have their own type of NPQ that was only recently discovered. Cyanobacterial NPQ is dependent on an orange carotenoid protein (OCP, *slr1963* gene) (Wilson, et al., 2006). OCP consists of an α-helical N-terminal domain and an α/β helical C-terminal domain, and it binds one carotenoid, a 3'-hydroechinenone molecule (Wilson, et al., 2010). OCP is the first discovered photoactive protein in which a carotenoid acts as a chromophore. The native OCP has two different forms, an inactive orange form and an active red form (Wilson, et al., 2008). The active form is induced by blue-green light that causes structural changes in the carotenoid. Hydroechinenone is inside of the structure of the OCP and has contact to both C and N terminal domains (Wilson, et al., 2010). OCP can also bind other carotenoids like echinenone and zeaxanthin (Punginelli, et al., 2009). However, binding of zeaxanthin leads to an inactive form of the OCP whereas binding of echinenone leads to an active form. This is due the lack of a carbonyl group in zeaxanthin (Punginelli, et al., 2009).

The active form of OCP attaches to the phycobilisome core APC_{660} (Tian, et al., 2012) and induces decrease in phycobilisome emission and reduces the amount of energy transferred to the PSII reaction center. In normal conditions wild type cells contain one OCP per two to three phycobilisomes, but different stresses can induce more OCP to the cells to help cells to acclimate (Gwizdala, et al., 2011). In contrast to plant NPQ, the cyanobacterial OCP-induced NPQ is temperature independent (Cadoret, et al., 2004).

The fluorescence recovery protein (FRP) has a central role in the separation of the OCP from the phycobilisome core (Boulay, et al., 2010). When FRP is affiliated to the active red form of OCP, the OCP separates from APC_{660} and turns to the orange inactive form (Boulay, et al., 2010). FRP is an essential protein in the recovery of the capacity of the phycobilisome antenna in dim light after exposure to high light (Boulay, et al., 2010). The amount of FRP in cells is probably considerably smaller than the amount of OCP (Boulay, et al., 2010).

Under iron deficiency, the PSI to PSII ratio decreases and simultaneously cells start to produce an iron deficiency protein named IsiA or CP43' (Bibby, et al., 2001). This Chl binding antenna polypeptide forms a ring structure around PSI and increases the light harvesting capacity of PSI (Kouril, et al., 2005). This leads to very efficient and active NPQ which replaces state transitions.

1.4.4. Adjustment of gene expression

Acclimation to new environmental conditions, like changes in the quantity or quality of light, requires changes in gene expression. Cyanobacteria have only one type of RNA polymerase that is responsible for all transcription. The cyanobacterial RNA polymerase holoenzyme consists of a catalytically active multi-subunit core and a sigma (σ) factor. The cyanobacterial RNA polymerase core consists of two identical α subunits, and β, β', γ and ω subunits (Schneider, et al., 1987; Schneider and Haselkorn, 1988). The σ factor recognizes specific promoter sequences, and each cyanobacterium contains multiple σ factors.

Cyanobacterial σ factors are σ^{70}-type, and have been divided into three subgroups according to structural and functional features (Lonetto, et al., 1992; Kaneko, et al., 1995; Imamura, et al., 2003). The group 1 σ factors are called primary σ factors because they are essential, and mainly responsible for transcription of housekeeping genes. The group 1 σ factor of *Synechocystis* PCC 6803 is SigA. The molecular weight of SigA is 67 kDa (Imamura, et al., 2003).

Group 2 σ factors of *Synechocystis* have a similar structure as the group 1 σ factor but they are non-essential, and they also have a smaller molecular weight from 40 to 47 kDa (Imamura, et al., 2003; Pollari, et al., 2008). Group 2 σ factors do not have a

conserved region 1.1, and the non-conserved region connecting conserved regions 1.2 and 2 are of variable length (Lonetto, et al., 1992). Models of *Synechocystis* group 2 σ factors visualize how similar group 1 and group 2 σ factors are (Pollari, et al., 2008). *Synechocystis* PCC 6803 has four group 2 σ factors, SigB, SigC, SigD and SigE.

The ΔsigB strain is fully viable and has a similar growth rate as the control strain in standard growth conditions (Imamura, et al., 2003; Tuominen, et al., 2006). In general, SigB seems to be involved in acclimation to several different kinds of stresses. The *sigB* gene is heat-shock responsive (Imamura, et al., 2003; Tuominen, et al., 2003; Tuominen et al., 2006,) and the transcription of a heat-shock gene *hspA* depends partly on the presence of SigB (Imamura, et al., 2003; Tuominen, et al., 2006). The ΔsigB strain is not able to acquire thermal tolerance as efficiently as the control strain (Tuominen, et al., 2006). In addition, SigB is involved in light acclimation processes. The SigB protein levels increased 2-fold after a shift from continuous light to darkness (Imamura, et al., 2003). The SigB mRNAs are very rapidly but only transiently induced when cells are transferred from dark to light (Tuominen, et al., 2003). SigB is also involved in the acclimation of the light harvesting systems to high light and in the regulation of *psbA* genes encoding the PSII reaction center protein D1 (Pollari, et al., 2009). Under nitrogen deprivation the SigB protein levels are circa 2 times higher, and SigB plays a central role in the NtcA-dependent nitrogen-related gene expression and regulates the expression of the *glnB* gene (Imamura, et al., 2006). Furthermore, transcription of the *sigB* gene is induced by osmotic (Paithoonrangsarid, et al., 2004), high salt (Marin, et al., 2003; Pollari, et al., 2008; Nikkinen, et al., 2012) and oxidative stresses (Kanesaki, et al., 2007).

The ΔsigC strain grows well in standard conditions, but shows retarded growth under mild heat stress (Tuominen, et al., 2008). The problems of the *sigC* inactivation strain in heat acclimation are partly dependent on the poor availability of inorganic carbon (Gunnelius, et al., 2010). The SigC factor has a role in acclimation to osmotic stress (Pollari, et al., 2008). SigC regulates genes of nitrogen metabolism during the stationary phase under nitrogen deprivation (Asayama, et al., 2004).

The ΔsigD strain has a similar growth rate as the control strain in standard conditions (Pollari, et al., 2008). The SigD factor accumulates in high light, and strains missing SigD grow slowly in high light (Imamura, et al., 2003; Pollari, et al., 2008). Normal activation of *psbA* genes in high light requires either the SigB or SigD factor (Pollari, et al., 2009). In addition, the SigD factor regulates nitrogen metabolism (Asayama, et al., 2004) and has also a small role in acclimation to salt and sorbitol-induced osmotic stress (Pollari, et al., 2008).

The fourth of *Synechocystis* group 2 σ factors, the SigE factor, is also involved in acclimation to salt-induced osmotic stress (Pollari, et al., 2008) and in nitrogen metabolism (Muro-Pastor, et al., 2001). Like the three other single inactivation strains, also the ΔsigE strain grows well in standard growth conditions (Pollari, et al., 2008). The SigE factor regulates genes involved in sugar catabolism (Osanai, et al., 2007). The SigE factor is under the control of circadian rhythm (Osanai, et al., 2005; Kucho, et al., 2005).

Synechocystis has four group 3 σ factors, SigF, SigG, SigH and SigI. These are also called as alternative σ factors. They are smaller than group 2 σ factors having molecular weight from 23 to 30 kDa (Imamura, et al., 2003). Usually group 3 σ factor proteins are not detected under normal growth conditions (Imamura, et al., 2003). SigG is essential but the physiological reason for that is not known (Matsui, et al., 2007). The SigI and SigH are non-essential, they are induced in many stress conditions but their actual physiological roles remain to be solved (Imamura, et al., 2003; Matsui, et al., 2007). SigF is the most intensively studied group 3 σ factor. SigF is needed for the formation of pili and for phototactic movements (Bhaya, et al., 1999; Asayama and Imamura, 2008).

2. AIMS OF THE STUDY

The first aim of this study was to investigate whether cyanobacteria are able to live and oxidize iron in conditions mimicking the Archaean ocean. I was also testing whether cyanotoxins have a role in iron tolerance.

In the theoretical part of the study, the aim was to solve the relationship between thermoluminescence, delayed light emission and Chl fluorescence during the charge recombination reaction $S_2Q_A^- \rightarrow S_1Q_A$, basing on the fact that the same thermodynamic parameters control the reaction in both fluorescence and luminescence. The results can be used as a tool for the analysis of thermoluminescence and fluorescence data. Additionally, a luminometer was brought into use for the first time and thus also the testing and optimizing of the luminometer were a parts of the work.

Fluorescence and luminescence methods were used for practical studies of *Synechocystis* σ factor mutants to see how different σ factors affect PSII.

3. METHODOLOGICAL ASPECTS

A number of methods ranging from growth measurements to TL, as well as different materials, were used to carry out the experiments. The main materials and methods used in this thesis are summarized in Table 1. As a general principle, each experiment described in the results sections of Papers I-V has been repeated by at least three times. The SE's are presented in growth curves when the error bar is larger than the data point (Papers I, IV and V). SE values of the fits of the TL data (Papers II and III) are not presented because the deviation of the model values from the experimental data tend to be largest at the beginning and end of the peak where the data are often affected by factors that are not included in the model. For this reason, the goodness of the fit was judged by visual comparison of the experimental data and the model. The TL curves of are averages of three very similar curves.

Table 1. Summary of materials and main methods. The bold headings identify the physiological phenomenon for which the methods were used.

	Paper				
Materials	I	II	III	IV	V
Nodularias spumigenia	X				
Microcystis aeruginosa	X				
Synechocystis sp. PCC 6803				X	X
Cucurbita maxima (pumpkin) thylakoids		X			
Spinacia oleracea (spinach) thylakoids			X		
Growth media					
Z8Y with different iron contents	X				
BG-11				X	X
Growth rate					
Chl *a* concentration	X				
A_{730}				X	X
IsiA induction					
77 K fluorescence	X				
NPQ					
Chl *a* fluorescence under blue-greenish light (PAM fluorometer)				X	
State transitions					
77 K fluorescence				X	X
Chl *a* fluorescence in darkness, blue and orange light (PAM fluorometer)				X	
Pigment composition					
Absorption spectra				X	X
Proteins, relations of PSII to PSI					
Western blotting				X	
$S_2Q_B^-$ recombination					
TL without DCMU (B-band)		X			
$S_2Q_A^-$ recombination					
TL in presence of DCMU (Q-band)		X	X		
TL (Q band) measured by varying flash energy		X			
Decay of Chl *a* fluorescence yield after a single turnover flash			X		

3.1. Plant and cyanobacteria material

Spinach (*Spinacia oleracea*) was grown at 24°C in 12 h light/12 h dark rhythm under the photosynthetic photon flux density (PPFD) of 250 μmol m^{-2} s^{-1} in Paper II and in the same light rhythm under the PPFD of 150 μmol m^{-2} s^{-1} at 20°C in Paper I. Pumpkin (*Cucurbita maxima*) was grown at 20°C in 16 h light/8 h dark rhythm under the PPFD of 150 μmol m^{-2} s^{-1} (Paper I). Thylakoid membranes were isolated as described earlier (Hakala, et al., 2005) and stored at -80°C.

I used several different cyanobacterial strains. In paper I, toxic AV1, GR8, BY1 and HEM and the non-toxic HKVV strains of the filamentous nitrogen fixing *Nodularia spumigenia* (hereafter *Nodularia*) were used. I also used the toxic *Microcystis aeruginosa* (hereafter *Microcystis*) strains NIES107 and the non-toxic strain PCC7005. In contrast to the filamentous *Nodularia*, the unicellular *Microcystis* is not able to fix nitrogen. *Microcystis* cells were grown in modified Z8 medium which did not contain tungsten, cadmium, chromium, vanadium or aluminum. This modified medium was named Z8Y. For *Nodularia*, 150 mM NaCl was added, and this medium was named Z8Ys. *Nodularia* was grown both in the presence and absence of nitrate. Iron tolerance experiments were done in aerobic (10-100 μM $FeCl_3$) and anaerobic (10-800 μM $FeCl_2$) conditions. Anaerobic conditions were generated inside a plexiglass box by nitrogen and CO_2 (3000 ppm) flow. This environment mimicked the atmosphere above the Archaean ocean. These experiments were done at 20°C in continuous light at PPFD 20 μmol m^{-2} s^{-1}.

The glucose tolerant strain of *Synechocystis* sp. PCC 6803 (Williams, 1988) (hereafter *Synechocystis*) was used as a control strain in papers IV and V. *Synechocystis* is a unicellular, non-toxic cyanobacterium and it is not able to fix nitrogen. In addition to the glucose tolerant strain, group 2 σ factor inactivation strains were used. The single inactivation strains ΔsigB (Tuominen, et al., 2006), ΔsigC (Tuominen, et al., 2008), ΔsigD (Tuominen, et al., 2006) and ΔsigE (Pollari, et al., 2008) were used in Paper IV. Four triple inactivation strains ΔsigBCD, ΔsigBCE, ΔsigBDE and ΔsigCDE (Paper IV) were used in Papers IV and V. Standard growth conditions for *Synechocystis* were: BG-11 medium supplemented with 20 mM Hepes pH 7.5, continuous PPFD 40 μmol m^{-2} s^{-1}, and 32°C. Liquid cultures were shaken at 90 rpm. All liquid cultures were grown without antibiotics, but the BG-11 agar plates of ΔsigBCD, ΔsigBCE, ΔsigBDE and ΔsigCDE were supplemented with kanamycin (50 μg/ml), streptomycin (20 μg/ml), spectinomycin (10 μg/ml) and chloramphenicol (10 μg/ml) and plates for the single activation strains with kanamycin (50 μg/ml).

3.2. Cyanobacteria growth experiments

Growth of the *Nodularia* and *Microcystis* strains was monitored by measuring Chl concentration after methanol extraction (Paper I). Cells were vacuum filtered to a glass microfilter. Chl *a* was then extracted by enclosing the filter in 1 ml of methanol for 24 h, and then measuring the absorbance of the solution at 665 nm and 750 nm. *Synechocystis* growth was monitored by measuring A_{730} (Papers IV and V). When cultures were dense, the samples were diluted so that A_{730} did not exceed 0.3. Dilutions were taken into account in final results. Different growth measuring methods were used because *Nodularia* is filamentous while *Synechocystis* is unicellular, and some *Nodularia* and *Microcystis* strains float in the growth medium while *Synechocystis* does not float.

Growth of *Synechocystis* strains was measured in standard conditions under continuous illumination (PPFD 40 µmol m^2 s^1) or under a 12 h light/12 h dark rhythm. For mixotrophic conditions, 5 mM glucose was added. Growth at the PPFDs of 20 and 80 µmol m^{-2} s^{-1} was also measured. Low temperature growth was followed at 22°C. For light quality experiments, cells were grown under blue or orange light at the PPFD of 40 µmol m^{-2} s^{-1} at 32°C.

3.3. Toxin and iron content measurements

The nodularin and microcystin contents were measured with HPLC (Meriluoto and Codd, 2005). The iron content was measured with the o-phenanthroline method (Vogel, 1962).

3.4. Absorbtion spectra (Paper IV)

In vivo absorption spectra of *Synechocystis* strains were measured with a UV3000 spectrophotometer (Shimadzu, Japan) from 350 nm to 800 nm.

3.5. Chl *a* fluorescence measurements

For assessment of NPQ and state transitions in *Synechocystis*, Chl *a* fluorescence was measured with pulse amplitude modulated (PAM) fluorometry (Papers IV & V). For NPQ measurements, samples were placed to a temperature controlled cuvette and dark incubated for 3 min. The F_0 level was measured with a weak measuring beam, and F_M was measured by using a saturating flash of 4 s and the PPFD of 5000 µmol m^{-2} s^{-1}.

The light-adapted maximum fluorescence level (F_M') was measured under illumination with blue-green light at PPFD 1000 μmol m^{-2} s^{-1} by firing saturating flash as at 40 s intervals. NPQ and state transition measurements were done at 32°C. Samples were first dark adapted for 3 min and after that illuminated for 135 s with blue-green light, PPFD 80 μmol m^{-2} s^{-1} (400 nm Corion long-pass and 500 nm Corion short-pass filters) and thereafter for 195 s with orange light, PPFD 20 μmol m^{-2} s^{-1} (600 nm Corion long-pass and 650 nm Corion short-pass filters). Saturating flashes during illumination were fired at 30 s intervals to measure F_M'.

For comparison of fluorescence with TL, the decay of Chl *a* fluorescence yield was measured in the presence of DCMU with FL-2000 fluorometer (Photon Systems Instruments, Brno, Czech Republic) at 0, 10, 20, 25, 30, 35 and 40°C (Paper III).

3.6. Emission spectroscopy (Papers I, IV & V)

To detect state transitions, 77 K emission spectra were measured with S2000 spectrophotometer (Ocean Optics) from in the control, ΔsigBCD, ΔsigBCE, ΔsigBDE and ΔsigCDE strains of *Synechocystis* (Papers IV & V). Cells were illuminated for 5 min with blue-green light (450 nm Corion short-pass filter) at PPFD 40 μmol m^{-2} s^{-1}, then kept in darkness for 5 min and after this illuminated again for 5 min with blue-green light. Samples were taken after each illumination step and frozen quickly with liquid nitrogen. Orange light (590 nm Corion narrow-band filter) was used for excitation of 77 K spectra.

Spectra were measured from cells treated with high iron to detect the possible expression of the iron-deficiency-induced IsiA protein (Paper I). The excitation wavelengths used in these measurements were 450 nm and 580 nm.

3.7. Thermoluminescence and delayed light emission

A homemade thermoluminometer was built to allow measurements of both TL and DLE. This was achieved by installing the photomultiplier tube on the sample in a slightly tilted position which allows a light guide to be inserted between the sample and a shutter protecting the detector. The sample cuvette was placed on top of a water cooled Peltier module that can cool and heat the sample between temperatures 20 and 70°C. The temperature was controlled with a fuzzy-logic-based software. Several different types of samples including leaf discs and thylakoids were used to measure TL for optimizing the function of the new luminometer. Different rates of cooling and heating (0.2 to 1.0°C/min) were tested to detect the intensity and position of the TL peak, and to test the actual

heating capacity of the device. The maximum heating rate was found to be 1°C/min. The details of the thermoluminometer are described in Paper II.

TL was measured in the absence (Paper II) and in the presence of 20 μM DCMU (Papers II & III) from pumpkin (Paper II) and spinach thylakoids (Papers II & III). DCMU is a plastoquinone analogue which blocks electron transfer from Q_A to Q_B by binding to the O_B site in photosystem II. The heating rate was 1°C/s. Samples were dark adapted for 15 min (Paper II) or 5 min (Paper III). The flash energy was 3.0 J in Paper III and in Paper II it was varied from 0.39 J to 4.44 J. The flash was given at -14°C (Paper II) or at -10°C (Paper III).

DLE was measured in the presence of DCMU at same temperatures as fluorescence (at 0, 10, 20, 25, 30, 35 and 40°C). The Chl concentration of thylakoid samples for DLE measurements was 200 μg Chl/ml. The samples were dark adapted for 5 min and DCMU was added like in the fluorescence measurements (described in detail in Paper III). The fast and slow components of DLE curves had to be measured with different amplifications (photomultiplier voltage -600 V for the fast and -800 V for the slow component). Both measurements lasted 130 s and the two data sets were then combined as DLE curve.

Differences in Chl concentration in TL and DLE measurements do not cause much difference in results because luminescence is measured from recombination reactions in complete darkness during heating (TL) or time (DLE), and the results are thereafter normalized.

3.8. Modelling (Papers II & III)

TL and fluorescence were modeled with ModelMaker software (ModelKinetics, Oxfordshire, UK). The models were compartment models where every reactant had its own compartment. Differential equations control the changes of the amounts of the reactants when the model is run. TL bands were simulated with equations by Arrhenius, Eyring and Marcus theories in Paper III. In Paper II, the Eyring theory was used as the basis of equations and the connectivity parameter J (Lavergne and Trissl, 1995) was taken into consideration.

3.9. Molecular biology methods (Papers IV & V)

To construct triple inactivation strains of group 2 sigma factors, inactivation plasmids pUC19-sigC-Cm^r and pUC19-sigE-Cm^r were constructed. The *sigC* or *sigE* gene

was amplified with PCR and cloned into pUC19. Then a fragment containing a chloramphenicol resistance cassette was obtained from pKRP10 and cloned into the middle of the *sigC* or *sigE* gene, and transformation of the double inactivation strains ΔsigBD, ΔsigBE and ΔsigDE was done. PCR analysis confirmed complete segregation of the inactivated genes. The details are described in paper IV. Western blotting was done to detect the amounts of the orange carotenoid protein, PSII reaction center protein D1 and PSI reaction center protein PsaA.

4. OVERVIEW OF THE RESULTS

4.1. Growth of cyanobacteria in media with high iron content

4.1.1. Growth medium Z8Y

Traditionally, W, Cd, Cr, V and Al have been added in low quantity to Z8 growth medium because natural waters contain traces of these toxic metals, but our growth experiments showed that they are not needed. Both *Nodularia* strains grew equally well with and without these metals (Paper I). The two cyanobacterial species had very different growth rates. In control conditions (10 μM Fe^{3+}) both *Microcystis* strains (PCC7005 and NIES107) grew faster than *Nodularia*.

4.1.2. Effect of high iron concentration in aerobic conditions

In present oceans, iron concentrations can often be so low that iron deficiency limits growth (Martin, 1990). However, in the distant past, concentrations of dissolved iron have been considerably higher than the current 0.03-2 nM (De Baar and De Jong, 2001; Parekh, et al., 2004). The standard growth media of cyanobacteria contain 10 μM iron. In this work, the iron tolerance of cyanobacteria was first tested in aerobic conditions by growing *Nodularia* and *Microcystis* at 5 to 10 times as high iron concentrations as in the standard growth media. The data indicate that the ability to produce toxins did not affect iron tolerance of *Nodularia* or *Microcystis* (Paper I). The toxic *Nodularia* strain AV1 died in 100 μM Fe^{3+} but the non-toxic HKVV grew fairly well. On the other hand, 100 μM Fe^{3+} had a stronger inhibitory effect on the growth of the non-toxic strain *Microcystis* PCC7005 than on growth of the toxic strain NIES107. 77 K fluorescence measurements showed that the iron-deficiency protein IsiA was not induced in high iron (Fig. 3A). Furthermore, the ratio between CP43 and CP47 to PSI was not affected significantly according to 77 K measurements (Fig. 3B).

Because the nitrogen fixing *Nodularia* can be grown with or without added nitrate, we tested if there are differences in iron tolerance when the medium contains nitrate or *Nodularia* is fixing nitrogen. *Nodularia* was found to tolerate 100 μM Fe^{3+} in the presence of nitrate; in the absence of nitrate, however, growth at 100 μM Fe^{3+} was drastically reduced (Paper I). 77 K fluorescence spectra revealed that different *Nodularia* strains can have quite different fluorescence spectra. However, the effects of excess iron were similar, including a rise of the phycobilisome peak (Fig. 3D). A fast change in

the form of the PSII fluorescence peak occurred when cells were grown in medium containing 100 µM Fe^{3+} (Figs. 3C, D). The spectra returned back to original form when cells adapted to high iron (Fig. 3D).

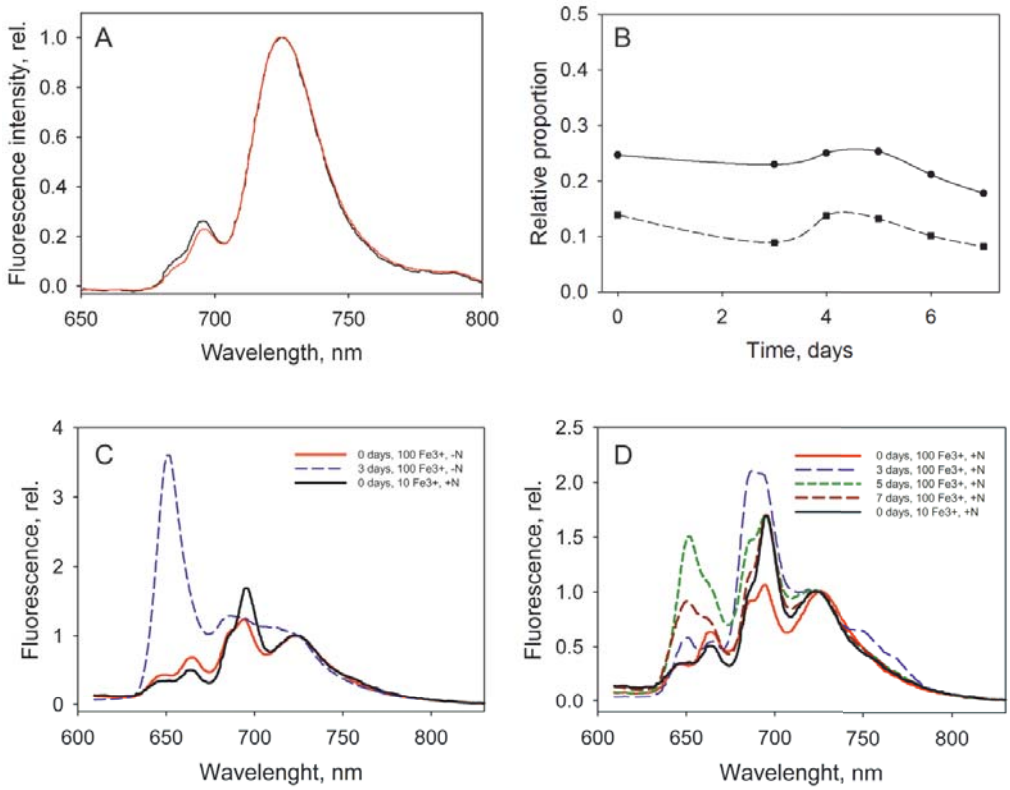

Figure 3. 77 K fluorescence measurements. A) 77 K emission spectrum from *Nodularia* HKVV grown with 10 µM (black) or 100 µM (red) Fe^{3+} for 4 days. Excitation was at 450 nm. B) Ratio of CP43 emission (dashed line) and CP47 emission (solid line) to PSI emission measured from *Nodularia* HKVV grown in the presence of 50 µM Fe^{3+}. Excitation was at 450 nm. C) 77 K emission spectrum from *Nodularia* HEM grown at 100 µM Fe^{3+} without nitrate (-N) and 10 µM Fe^{3+} with nitrate (+N). D) 77 K emission spectrum from *Nodularia* HEM grown at 100 µM Fe^{3+} with nitrate (+N) and at 10 µM Fe^{3+}. Excitation was at 580 nm both in C and D.

4.1.3. High iron concentration in anaerobic conditions

Next we tested iron tolerance in anaerobic conditions mimicking the conditions in the Archaean ocean. In anaerobic conditions, all strains tolerated much higher iron concentrations than in aerobic conditions. The non-toxic *Nodularia* strain HKVV was able to grow in as high concentration as 650 µM Fe^{2+} and died only at 800 µM Fe^{2+}. The toxic strain AV1 stayed alive and grew slowly in 150 µM Fe^{2+} but died at 300 µM Fe^{2+}.

Both *Microcystis* strains tolerated high iron concentrations, and the non-toxic PCC 7005 grew slightly faster than the toxic NIES107 in 300 μM Fe^{2+}. In 650 μM Fe^{2+}, PCC7005 was still able to grow but NIES107 died. Like HKVV, PCC7005 died in 800 μM Fe^{2+} (Paper I).

4.1.4. Iron oxidation

Because BIFs were formed from O_2 and ferrous iron, we studied whether cyanobacteria are able to form this kind of sediment in anaerobic growth conditions. Oxygen produced by cyanobacteria in growth vessels was found to react with ferrous iron and to lead to brown sedimentation on the bottom of the vessels. In a 50 ml culture of PCC7005 in 650 μM Fe^{2+}, the sediment contained 0,3–0,4 μmol iron after ten days of growth. In same time, photosynthesis produced 0.25 mg (20 μmol) of new Chl (Paper I) and so approximately 25 mg carbon was assimilated, assuming that the carbon:Chl ratio is 100 (Wang, et al., 2009). Thus less than 2 % of the oxygen produced during growth reacted with iron; the rest must have escaped from solution.

4.2. Analysis of thermoluminescence, fluorescence and delayed light emission

4.2.1. Energy transfer between PSII centers affects thermoluminescence

Paper II aimed at elucidating the effect of energetic connectivity of PSII on the Q band of TL. The topic had not been earlier discussed in the literature. The experimental Q band was first compared with two kinetic models, a pure first order kinetic model and another where the connectivity parameter J was taken into account (Paper II). The model with the connectivity parameter fitted better to the experimental data. The simulations of the changes of J values showed that increasing J leads to a wider and more symmetrical TL band, and the simulated peak shifts toward a lower temperature. The effect of the initial fraction of closed PSII centers was tested by measuring TL in the presence of DCMU from pumpkin and spinach thylakoids by using different intensities of the excitation flash. When flash intensity was changed from saturating (100 %) to 0.39 % of saturation, the TL Q band peak position moved ~2.5°C toward a higher temperature. Simultaneously, the area of the TL peak decreased from 100 % to 3.2 %.

In the experiment above, the flash was fired at -14°C during heating (1°C/s). Applying a 30 s delay between the exiting flash and the beginning of the heating led to lower TL bands. In this case, lower flash intensities did not lead to clearly narrower bands or

clear movement of the peak position. However, the form of the Q band still resembled a second-order TL band.

In terms of the reaction pathways, the analysis in Paper II was done assuming that the luminescence-producing reaction is the only pathway of recombination, or that other pathways do not significantly affect the form of the TL peak. This assumption is called the "deactivation" model of analysis of TL (Lavorel, 1975).

4.2.2. Analysis of thermoluminescence and fluorescence originating from the $S_2Q_A^-$ recombination reaction

The Q band of TL of pumpkin thylakoids peaked at 17°C. After the Q band TL intensity increased again, suggesting the presence of another TL peak above 60°C.

In terms of the reaction pathways of charge recombination, the TL analysis in Paper III was based on the Rappaport-Lavergne model (Rappaport and Lavergne, 2009). Thus, a deactivation-type analysis of TL used in Paper II was changed to a "leakage"-type scheme in Paper III, as only a small fraction of $S_2Q_A^-$ recombinations were assumed to produce luminescence, and it was assumed that the three routes of recombination compete for the same substrate. In modeling the rate constants of the pathways, the Arrhenius, Eyring and Marcus theories were used. The results showed that the Marcus theory gave the best fit, the Arrhenius equation gave the poorest one, and the Eyring equation was slightly better than the Arrhenius equation. In the model, PSII was divided to a fast population (a rapidly recombining population of PSII centers) and a slow population (slowly recombining population of PSII centers). The amount of the slow population in the TL analysis was kept at 75 % for all three theories.

Fluorescence was measured in the presence of DCMU at different temperatures. The decay of Chl *a* fluorescence yield occurred faster at higher temperatures. In fluorescence analysis, the fractions of the fast and slow PSII populations varied between temperatures. The very slow component of fluorescence decay was successfully fitted with the parameters of the high-temperature band of the TL curve. The amplitude of this very slow phase in fluorescence decay was 13–32 %. The activation parameters obtained by using the three different theories are tabulated in Paper III, Tables 1, 2 and 3.

4.2.3. Delayed light emission

DLE was measured in the presence of DCMU at same temperatures as fluorescence. However, it was not possible to analyze DLE with the same models as TL and fluorescence. The simulated TL model did not fit to the DLE curves, suggesting that there are more components in DLE than in TL.

4.3. Triple inactivation strains of group 2 sigma factors of *Synechocystis* sp. PCC 6803

Three out of four group 2 σ factor genes were inactivated simultaneously, and the resulting *Synechocystis* strains contained only one functional group 2 σ factor; SigE in ΔsigBCD, SigD in ΔsigBCE, SigC in ΔsigBDE and SigB in ΔsigCDE. In standard growth conditions (continuous light PPFD 40 μmol m^{-2} s^{-1}, 32°C), the autotrophic growth of all triple inactivation strains was similar to that of the control strain, and in accordance with that, light saturated photosynthetic activities of all strains were similar. Absorption spectra measurements revealed that control, ΔsigBCD, ΔsigBCE and ΔsigBDE strains have similar spectra, indicating that phycobilin to Chl *a* and carotenoids to Chl *a* ratios were similar in these strains (Fig. 4). Furthermore, it was shown by measuring the amounts of the reaction center proteins D1 (PSII) and PsaA (PSI) that the PSII:PSI ratio was similar in the control and ΔsigBCE strains. The ΔsigCDE strain had a similar phycobilin to Chl ratio as the other strains but the carotenoid peak was higher than in the other strains (Fig. 4).

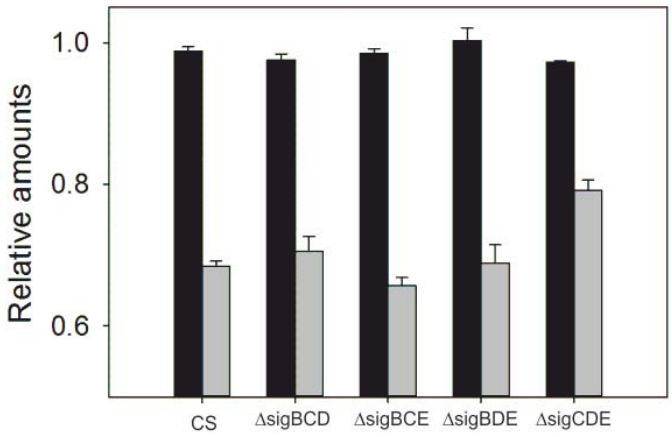

Figure 4. Phycobilin to Chl *a* (black) and carotenoid to Chl *a* (grey) ratios in the control and σ factor triple inactivation strains of *Synechocystis*.

In addition to normal autotrophic growth, the glucose tolerant strain of *Synechocystis* can grow in the presence of 5 mM glucose in the light. The control and all other triple inactivation strains except for ΔsigBCD grew faster in mixotrophic than in autotrophic conditions (Paper IV).

When temperature was decreased from the standard 32°C to 22°C, the growth of the control strain was slow, the doubling time being circa 19 h (in standard conditions circa

12 h). At 22°C, the triple inactivation strains ΔsigBCD and ΔsigBDE and the single inactivation strains ΔsigB and ΔsigD grew slowly compared to the control strain while ΔsigBCE and ΔsigCDE grew as fast as the control strain. In 12h light/12 h dark light rhythm at 22°C, ΔsigBCD and ΔsigBDE were not able to grow almost at all, while ΔsigCDE and ΔsigBCE grew only slightly more slowly than the control strain. At 32°C, the light rhythm did not have any effect on the growth of the inactivation strains compared to the control strain (Paper IV). Light rhythm clearly enhanced the low temperature sensitive phenotypes of ΔsigBCD and ΔsigBDE but a similar effect was not detected in ΔsigB or ΔsigD. According to these results, the presence of either SigB or SigD seems to be important to acclimation to low temperature.

4.3.1. Acclimation to blue light

The growth of ΔsigBCE in blue light (40 μmol m^{-2} s^{-1}) was slower than that of the control strain or other triple inactivation strains. This difference was a blue light specific phenomenon, as similar growth was obtained in orange and white light (Paper IV). Because cyanobacterial NPQ is induced by blue-green light and the ΔsigBCE strain grew slowly in blue light, the OCP content and NPQ were studied. Western blot results showed that the OCP content was slightly higher in ΔsigBCE than in the control strain after one hour of blue or high light treatments (Paper IV). However, there were no differences in the blue light induced NPQ between the ΔsigBCE and control strains (Paper IV). As NPQ did not explain why the ΔsigBCE strain was not able to grow like the control strain in blue light, the state transitions were studied.

State transitions were induced by light treatments. In darkness, cyanobacterial cells are in state 2, and blue light illumination causes a change to the high fluorescence state 1. Orange light, in turn, causes a change to state 2. For the 77 K measurements, samples were first taken directly from growth conditions, and then another sample was taken after a 5-min blue-light illumination, a third one after a 5-min dark adaption, and the last one after a new 5-min illumination in blue light. The 77 K fluorescence measurements revealed that the ΔsigBCE strain does not have as clear state transitions as the control strain and seems to be locked in state 1. This phenomenon was confirmed by results obtained with a PAM fluorometer (Paper IV). In these experiments, F_M' was measured in darkness, then during illumination with blue light and after that during illumination with orange light, and finally again in darkness. The control strain showed a clear state 2 to state 1 transition after transfer from dark to blue light and a state 1 to state 2 transition when light was changed from blue to orange. The ΔsigBCE strain, however, did not show state transitions but it appeared to be locked in state 1. All other group 2 σ factor triple inactivation strains had higher PSII fluorescence peaks (both 683 nm and 693 nm)

than the control strain (Table 2) (Paper V). This finding may suggest that the lack of state transitions in the ΔsigBCE strain is an extreme case of a similar phenomenon in all triple inactivation strains.

Table 2 Intensities of the peaks of CP43 (683 nm) and CP47 (693 nm) in 77 K emission spectra of triple inactivation strains. The peaks have been normalized to the PS I emission peak at 725 nm. The spectra were measured from cells taken directly from growth (GL) conditions and after 5 min of blue light (BL) illumination. Orange light was used for excitation.

	CS		ΔsigBCD		ΔsigBCE		ΔsigBDE		ΔsigCDE	
	GL	BL	GL	BL	GL	BL	GL	BL	GL	BL
CP43 (683 nm)	0.75	0.84	1.02	1.07	0.95	0.98	0.82	0.95	0.88	0.92
CP47 (693 nm)	0.86	0.95	1.11	1.13	1.06	1.06	0.99	1.06	1.00	1.08
CP43/CP47	0.87	0.89	0.92	0.95	0.90	0.92	0.89	0.90	0.88	0.85

4.3.2. Acclimation to different light intensities and photoinhibition

At PPFD 20 μmol m^{-2} s^{-1}, all triple inactivation strains grew slightly more slowly than the control strain, and at PPFD 80 μmol m^2 s^1 ΔsigBCD and ΔsigBDE were not able to grow as well as the control strain but ΔsigBCE and ΔsigCDE enhanced their growth like the control strain (Paper V). Obviously *Synechocystis* cells lacking SigB and SigD simultaneously were not able to use higher light as efficiently as the control strain.

Photoinhibition was measured at PPFD 1500 μmol m^{-2} s^{-1}. In the ΔsigBCD, ΔsigBCE and ΔsigBDE strains, photoinhibition was 20 % faster than in the control strain whereas ΔsigCDE behaved like the control strain (Paper IV). The only group two σ factor left in the ΔsigCDE strain is SigB which seems to be important for high light acclimation.

5. DISCUSSION

5.1. Cyanobacteria tolerate high iron concentrations in anaerobic but not in aerobic conditions

In paper I, toxic and non-toxic cyanobacteria were grown with excess iron. The results confirm that cyanobacteria are able to live in anaerobicity and high iron concentrations, which were typical conditions in Archaean oceans. The results also showed that cyanobacteria are capable of causing the precipitation of iron oxides in these conditions, and thus it is possible that cyanobacteria caused the formation of BIFs.

Only 1 % of the oxygen produced in the growth vessel had reacted with iron after ten days of growth, indicating that the main part of oxygen escaped to the atmosphere from the cultivation. This may suggest that oxygen would have escaped to the atmosphere from the very beginning of the existence of oxygen-evolving photosynthetic cyanobacteria. However, geochemical evidence shows that cyanobacteria existed already in the time range 3.4 to 2.8 BA (Schopf and Packer, 1987; Schopf, 1993; Summons, et al., 1999) whereas the first evidence of the rise of the oxygen content of atmosphere is from 2.45 BA (Bekker, et al., 2004; Claire, et al., 2006). Thus, cyanobacteria of the Archaean ocean must have lived in relatively deep waters, which would explain why the oxygen that they produced reacted with Fe^{2+} rather than escaped to the atmosphere. Another possible reason why cyanobacteria may have favoured deep waters is that there was no protective ozone layer during the Archaean era. Water absorbs UV-light more efficiently than photosynthetically active light. Even nowadays, some cyanobacteria are found as deep as 140 m in oceans (Zubkov, et al., 2000). Obviously, oxygen produced in depths reacted with iron, which led to the formation of iron precipitates. Only after the iron content in waters had been lowered, oxygen started to escape to the atmosphere, which led to the formation of a protective ozone layer. Habitation of surface waters was then possible.

The above scheme can be criticized by noting that all geologists do not assume that the oxygen content of the atmosphere depends on the rate of oxygen production. In an alternative scheme, oxygen levels increased first about 3.0 BA, decreased then again about 0.2 BA later (Ohmoto, et al., 2006), and Earth's atmosphere was bistable for some time before the great oxidation event which may have been caused by a 3 % increase in burial of organic carbon (Goldblatt, et al., 2006).

The estimated yearly iron precipitation in BIFs was 45.3 mol Fe m^{-2} (Konhauser, et al., 2002) which would not be reached by the rate of current day primary production

in oceans (11.7 mol C m^{-2} $year^{-1}$) (Field, et al., 1998). However, the rate of current day primary production in oceans is limited by shortage of iron in seawater (Martin, 1990; Loukos, et al., 1997) and therefore primary production may have been considerably faster in Archaean oceans.

Another important finding of Paper I was that excess iron is much more toxic to cyanobacteria in aerobic conditions than in anaerobic conditions. This may indicate that excess iron is toxic because iron ions induce the production of reactive oxygen species. Furthermore, the nitrogen fixing *Nodularia* tolerated higher iron concentrations under aerobic conditions when the medium contained nitrate (Fig. 3C, D). This finding may indicate that reactive oxygen species specifically affect the heterocysts or interfere with the interaction between vegetative cells and heterocysts.

Fluorescence measurements at 77 K (Figs. 3C, D) confirmed that the fluorescence spectra of toxic and non-toxic *Nodularia* strains are different (Keränen, et al., 2009). The main difference is the PSII/PSI ratio which is circa 1.5 in the non-toxic and circa 2 in the toxic strains (Keränen, et al., 2009). This ratio is compatible with our results, as in the non-toxic strains the PSII/PSI ratio varied between 0.9 and 1.1, whereas in the toxic strains the ratio was 1.7 to 2.3. Exposure to excess iron caused a rapid appearance of a high phycobilisome peak in the fluorescence spectra (Figs. 3C, D). The high phycobilisome peak could be due to the presence of free phycobilisomes (Figs. 3C, D). The measurements also showed that in a few days, the spectra returned to normal in cells that tolerated the high iron content.

One of the aims of Paper I was to test the possible importance of cyanotoxins in iron metabolism. In Paper I, the toxins did not offer any protection in excess iron conditions. In the literature, iron deficiency has been studied much more than excess iron. The main effect of iron deficiency in cyanobacteria is the accumulation of the IsiA chlorophyll-protein complex (Bibby, et al., 2001); iron deficiency also causes monomerization of PSI trimers and reduces the capacity of state transitions (Ivanov, et al., 2006). It has been proposed that microcystins can protect cells against reactive oxygen species during iron starvation (Alexova, et al., 2011), and microcystin production has also been found to be suppressed (Utkilen and Gjolme, 1995) as well as induced (Lukac and Aegerter, 1993) by iron deficiency. In our experiments, neither excess iron nor iron deficiency induced toxin production. Thus, the results of Paper I do not support the hypothesis that the toxins are involved in iron metabolism.

5.2. A common model for analysis of thermoluminescence and fluorescence associated with the $S_2Q_A^-$ recombination reaction

When TL is modeled, three different theories for reaction rate have been applied. The Arrhenius equation of reaction rate is commonly used (Rappaport and Lavergne, 2009) although it has not been developed for dealing with reaction rates of electron transfer reactions. Another theory used to calculate activation energies of reactions is the Eyring theory which has been designed for the analysis of reactions between gas molecules (Glasstone, et al., 1941). The Eyring theory has also been used to analyze photosynthetic TL (Vass, et al., 1981; Demeter and Vass, 1984; Demeter, et al., 1985; Hakala-Yatkin and Tyystjärvi, 2011). The Marcus theory is specifically designed for electron transfer reactions (Marcus and Sutin, 1985), and therefore it can be expected to be the best tool for the analysis of TL.

5.2.1. Connectivity of PSII and thermoluminescence

The shape of the fluorescence induction curve of thylakoids, measured in the presence of DCMU, can be interpreted by assuming that PSII centers can transfer energy to each other (Joliot and Joliot, 1964; Lavergne and Trissl, 1995). The phenomenon is called PSII connectivity. The analysis of Paper II tested the hypothesis that PSII connectivity should also affect the shape of the TL Q band. The reason why energetic connectivity would affect TL, is the same as in the analysis of TL from semiconductors, described already in 1946 by Garlick and Gibson (Garlick and Gibson, 1948). Semiconductor luminescence is described with traps and luminescence centers. The traps are analogous to the charge separated states in PSII, and the luminescence center corresponds to the ground state. In semiconductors, the valence band is common to all luminescence centers and to all semistable trap states. Therefore, an electron raised to the valence band will drop to a luminescence center if all semistable traps are occupied, but may easily enter a trap without producing luminescence if the traps are unoccupied. Similarly, the fraction of closed PSII centers affects the peak position of the Q band, and this must in general be taken into account in TL measurements. However, if the flash used to separate the charges is not saturating, then the effect of connectivity is negligible (Paper II)

The model used in the analysis of TL connectivity was the connected-units model (Lavergne and Trissl, 1995) and for the reaction rate constant, the Eyring equation (Eq. 4) was used. The connectivity was taken into account through the parameter J (Paper II, equation 10) (Lavergne and Trissl, 1995). This correction makes the simulated Q band resemble a second-order TL band. The J value was 0.4 for both pumpkin and spinach thylakoids. This value is similar to values obtained from leaves of higher plants (Strasser

and Stirbet, 2001) but lower than values obtained from spinach thylakoids in fluorescence measurements (Kirchhoff, et al., 2004).

5.2.2. Association of thermoluminescence and fluorescence with recombination reactions of PSII

TL and fluorescence are two different methods that can be used for measuring the recombination reactions of PSII. TL measures the activation parameters more directly, as the intensity of TL is proportional to the rate of the luminescence -producing pathway of the recombination reaction $S_2Q_A^- \rightarrow S_1Q_A$ at any moment, whereas the quantum yield of fluorescence is proportional to the fraction of the reactant $S_2Q_A^-$. The rate of the decrease of the fluorescence yield depends on temperature. Because the form of the TL band and the decay of fluorescence yield reflect the same recombination reactions, the same activation parameters are expected to control these phenomena.

In Paper II, TL was treated as if all recombination reactions of $S_2Q_A^-$ produced luminescence. This is called as the "deactivation" model. However, the recombination may proceed via multiple, alternative routes (Rappaport, et al., 2002; Rappaport, et al., 2005). In this so called "leakage" model only one reaction route produces luminescence whereas other routes are non-luminescence producing. This multiple-reaction-route model seems to be needed to explain the shape of TL Q band even though the dependence of peak position and relative width are also affected by the energetic connectivity of PSII. Multiple reaction routes may be behind the lower J values obtained from TL (Rappaport, et al., 2002; Rappaport, et al., 2005). A similar apparent loss of the effect of connectivity was seen when the initial fraction of PSII centers in the $S_2Q_A^-$ state was lowered by applying a 30-s delay between the flash and the start of heating (Paper II). Such loss of the effect of connectivity is obviously caused by a non-excitonic recombination reaction that proceeds at low temperature. Such a reaction must have a low activation energy but also a low pre-exponential factor. As discussed below, these features are compatible with the characteristics of the "direct" recombination route (Rappaport and Lavergne, 2009)

In Paper III, TL and fluorescence, at different temperatures, were measured in the presence of DCMU to create a common model to be used for the analysis of the results of these two methods. The reaction route model used in this study is the Rappaport & Lavergne leakage type TL scheme (Rappaport, et al., 2002; Rappaport, et al., 2005; Rappaport and Lavergne, 2009). According to this three-route model (Fig. 5), recombination of $S_2Q_A^-$ can occur via three different routes. In the "direct" and "indirect" routes, free energy is lost as heat whereas the "excitonic" route leads to an exited state of the primary donor and may therefore produce luminescence. The excitonic route accounts for only 3 % of the overall decay, as the indirect and direct routes account for

77 % and 20 % of overall decay, respectively (Fig. 5). The route is called indirect when an electron is transferred via $Pheo^-$ and direct when the electron goes directly from Q_A^- to P_{680}^+.

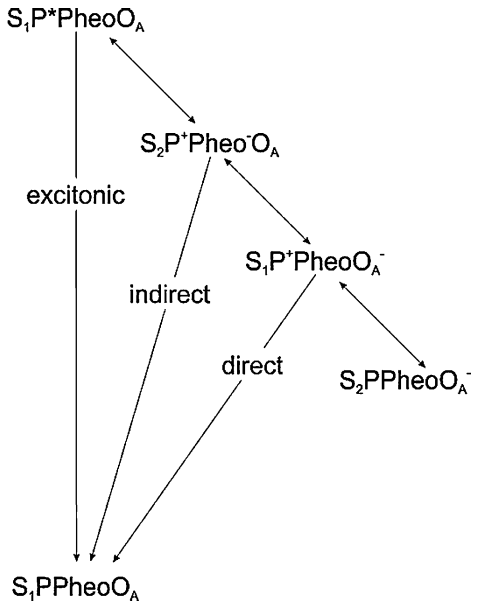

Figure 5. The main recombination routes of $S_2Q_A^-$. Only the excitonic route produces luminescence. The scheme is drawn according to Rappaport and Lavergne (2009).

5.2.3. Comparison of Arrhenius, Eyring and Marcus theories in $S_2Q_A^-$ recombination reaction

Three different reaction rate theories, Arrhenius, Eyring and Marcus theory, were compared with each other to test which gives the best fit for the combined fitting of the TL and fluorescence data. The results showed that compromises were needed to keep the fitting-error in both TL and fluorescence reasonable. The Marcus theory gave the best fit whereas the commonly used Arrhenius equation gave the poorest fit. However, it was found that all three theories can be used to simultaneously analyze TL and fluorescence. The Arrhenius theory gave the same (s_0) or very similar values (E_a) for the thermodynamic parameters as previous studies (Rappaport and Lavergne, 2009). Also the Eyring theory was found to lead to similar results as an earlier study that used a similar model (Hakala-Yatkin and Tyystjärvi, 2011). In an earlier study in which the Eyring theory was used with a deactivation type model, slightly smaller ΔH_a (720 meV) and ΔG_a (810 meV) values and also a smaller ΔS_a value (-0.318 meV/K) was obtained (Vass, et al., 1981). For Marcus theory, there are no previous photosynthetic

TL studies to compare with. However, parameter values obtained by the fitting are physically reasonable in comparison to literature on other electron transfer reactions of PSII (Haffa, et al., 2002; Moser, et al., 2006). The results may suggest that the Marcus theory should be used to analyze of TL data. However methods need to be developed to handle each reaction of the reaction chain separately, as Marcus theory requires more detailed treatment of the reaction series than the Arrhenius equation.

The TL data revealed a second TL band at a higher temperature than the Q band. The fitting of the decay of Chl *a* fluorescence yield after single turnover flash revealed a component with exactly the same thermodynamic parameters as in the high-temperature-TL band, strongly suggesting that the same reaction is seen in both data. The finding that the component can be seen in fluorescence indicates that Q_A^- recombination is involved in this component. The component may be associated with inactive PSII centers.

In the three-routed model (excitonic, indirect and direct route) (Rappaport and Lavergne, 2009) PSII is divided to fast and slow recombining populations. The fractions of the fast and slow component varied in different temperatures in fitting of fluorescence, and it may be that there is temperature dependent equilibrium between these two conformations of PSII. The effect of PSII connectivity (Paper II) was minimized in Paper III by using a weak actinic light for TL.

The Arrhenius, Eyring and Marcus theories were also compared with regard to the values of the pre-exponential and exponential factor. The Marcus theory was found to give higher values of the pre-exponential factor than Arrhenius and Eyring equations. On the contrary, values of the exponential factor were smaller in the Marcus theory than in Arrhenius and Eyring theories.

In further studies it should be taken into account that $S_2Q_A^-$ recombination consists of several component reactions. When TL and fluorescence are fitted independently from each other, the fitting can lead to different factor values. When they are modeled simultaneously, the modeling error decreases. The results of fitting are even more reliable when fluorescence is fitted at several different temperatures. The best theory for describing these factors is the Marcus theory which is a special theory for electron transfer reactions unlike the commonly used Arrhenius theory.

5.3. Fluorescence studies reveal differences in light acclimation of group 2 sigma factor inactivation strains

All triple inactivation strains, ΔsigBCD, ΔsigBCE, ΔsigBDE and ΔsigCDE, are able to grow like the control strain in our standard growth conditions. Furthermore, the simultaneous inactivation of three group 2 σ factors does not affect the photosynthetic

activity under standard growth conditions. The biophysical methods made it possible to analyze light harvesting and photosynthetic properties of the strains in more detail when cells were acclimated to different light intensities and qualities. These studies revealed that group 2 σ factors are important in light acclimation responses.

Expression of σ factors is light responsive. Only low amounts of *sigA*, *sigB*, *sigC*, *sigD* and *sigE* transcripts were detected after 18 h of dark treatment (Tuominen, et al., 2003). When cells were grown in 12 h light/12 h dark rhythm, circa 350 genes were differently (at least 1.5 fold change) regulated in ΔsigD and CS in the light, and 149 genes in the dark (Summerfield and Sherman, 2007). In darkness, absence of SigB affects the transcription levels of over 150 genes (Summerfield and Sherman, 2007). There are controversial results about induction of SigB in light-dark transitions. High, but only transient upregulation of *sigB* mRNA was detected upon a dark to light transition (Tuominen, et al., 2003) while the level of the SigB protein was found to decrease during dark to light transition (Imamura, et al., 2003). It should be noted that the high *sigB* transcript levels were measured immediately after the dark to light transition (Tuominen, et al., 2003) while protein levels were measured only an hour after the dark to light sift (Imamura, et al., 2003). After an hour, also the amount *sigB* mRNA returns to a low level.

The SigE factor is also involved in regulation of responses to light-to-dark transitions in *Synechocystis* (Osanai, et al., 2009). In the light, the ChlH anti-σ factor bounds to *sigE* inactivating it. Upon transfer of cells to darkness, the cellular Mg^{2+} concentration decreases, causing dissociation of ChlH from SigE (Osanai, et al., 2009). All triple inactivation strains grew as well as the control strain under 12 h light/12 h dark rhythm at 32°C. However, application of a light rhythm together with low temperature enhanced low temperature phenotypes of the mutant strains. The finding that the growth rates of the triple inactivation strains were slower (ΔsigBCE and ΔsigCDE) or they were not able to grow almost at all (ΔsigBCD and ΔsigBDE) under diurnal light rhythm at 22°C may indicate that sigma factors may also be involved in regulation of circadian rhythms. The expression of SigE shows a diurnal light rhythm (Osanai, et al., 2005).

Previous studies have shown that s*igD* is upregulated under high light conditions (Hihara, et al., 2001; Huang, et al., 2002; Imamura, et al., 2003), and the corresponding gene *rpoD3* in *Synechococcus* sp. PCC 7942 is also upregulated in high light (Seki, et al., 2007). The mutant strains ΔsigBCD and ΔsigBDE were not able to enhance their growth at PPFD 80 μmol m^{-2} s^{-1} light like the control strain. Strains ΔsigBCD and ΔsigBDE are lacking SigB and SigD factors simultaneously, and the ΔsigBD strain has earlier been shown to be unable to enhance growth rate when the growth light was doubled (Pollari et al., 2008). Furthermore, all double mutants lacking SigD and also the ΔsigD strain are sensitive to bright light (Pollari et al., 2008).

Under mixotrophic conditions the control, ΔsigBCE, ΔsigBDE and ΔsigCDE grew faster than in autotrophic conditions. The growth of the ΔsigBCD strain (having only *sigE*) was similar in both conditions. The SigE factor has been previously showed to be involved in regulation of sugar catabolic pathways and to be important for light activated heterotrophic growth (Osanai, et al., 2005; Summerfield and Sherman, 2007). It may be that when present as the only group 2 σ factor, SigE is recruited more often to form the RNA polymerase holoenzyme. This situation can lead to interference of sugar metabolism, which may cause an inability to enhance growth by efficient use of glucose from the growth medium.

In blue light, the ΔsigBCE strain grew slowly and was not able to perform state transitions. The ΔsigBCE strain is locked to state 1. In fact, all triple inactivation strains have a higher PSII peak in the 77 K fluorescence curves than control strain. These data may suggest that all triple inactivation strains are constantly near to state 1, although only the ΔsigBCE strain is fully locked to state 1. This finding suggests that an association between phycobilisomes and PSI may depend on the presence of group 2 σ factors. In ΔsigBCE, phycobilisomes cannot associate with PSI at all, but in the other triple inactivation strains, the association of phycobilisomes with PSI occurs less efficiently than in the control strain. Thus, the group 2 σ factors appear to have overlapping roles in the state transitions. An inactivation strain of RpaC (regulator of phycobilisome association C) is locked to state 1. The RpaC mutant has a normal phenotype in standard conditions, but at very low light it grows more slowly than the control strain (Emlyn-Jones, et al., 1999). Interestingly, also all triple inactivation strains grow slowly at PPFD 20 μmol m^{-2} s^{-1} (Paper V). Importance of state transitions in low light has been earlier suggested (Emlyn-Jones, et al., 1999). No difference between the control and the ΔsigBCE strain were detected in the blue-light induced, OCP-related NPQ (Wilson, et al., 2006). This finding is in line with previous results showing that OCP-related NPQ and state transitions are separate phenomena (Wilson, et al., 2006; Wilson, et al., 2007; Wilson, et al., 2008; Wilson, et al., 2010).

Recently it has been proposed that cyanobacteria have a previously unknown photoprotection mechanism involving the *flv4-flv2* operon (Zhang, et al., 2009; Zhang, et al., 2012). Also the *flv4-flv2* operon mutants have a higher PSII peak than the control strain. However, ΔsigBCD, ΔsigBCE, ΔsigBDE and ΔsigCDE have relative proportions of CP43 and CP47 similar to control strain (Table 2) unlike the *flv4-flv2* operon mutant that has a high CP43 peak at 685 nm compared to the 695 nm peak. The ΔsigCDE strain is resistant to photoinhibition. Depending on light intensity, the light-induced damage of PSII occurs 30 to 50 % more slowly in ΔsigCDE than in the control strain (Hakkila et al. manuscript). A high carotenoid content together with up-regulation of *flv4-flv2*

operon are the most important reasons for photoinhibition resistance of ΔsigCDE strain (Hakkila, et al., manuscript). In some of the previous studies, SigB has consider to be more important in darkness than in the light (Imamura, et al., 2003) but recent results from the ΔsigCDE strain prove importance of the SigB factor in light.

Studies of the ΔsigCDE strain in high salt conditions have revealed that the SigB factor also regulates many salt acclimation responses in *Synechocystis* (Nikkinen, et al., 2012). The protective carotenoids zeaxanthin and myxoxanthophyll are upregulated in the control strain in high-salt conditions but in the ΔsigCDE strain these carotenoids are already up-regulated in normal conditions (Nikkinen, et al., 2012). The SigB factor is also important for the production of glucosylglyserol-phosphate synthase and the HspA heat shock protein in high salt conditions (Nikkinen, et al., 2012).

Overall group 2 σ sigma factors have a central role in the global regulation of transcription in cyanobacteria. The competition for the binding of group 2 sigma factors to the RNA polymerase core might play a key role in the regulation of gene expression in *Synechocystis*.

6. CONCLUSIONS

My thesis consists of a theoretical part (Papers II and III) and a more applied part (Papers I, IV and V). When trying to resolve the function of specific genes, proteins or pathways, it is useful also to understand the environment where the organism has evolved, and the effect of the environment to the organism (Paper I). Understanding of gene regulation in a present-day organism (Papers IV and V) benefits from the knowledge of the past. The main findings of my thesis are:

- The peak temperature and form of the Q band of PSII thermoluminescence depend on the initial concentration of Q_A^-, indicating that energy transfer between PSII centers affects thermoluminescence
- The connected units model of PSII organization describes the effect of the energy transfer between PSII centers
- The Marcus theory gives a better fit in modeling PSII thermoluminescence and fluorescence than the Arrhenius or Eyring models
- Three out of four group 2 σ factors can be inactivated simultaneously without affecting growth in standard conditions but biophysical studies revealed differences between the strains
- ΔsigBCE grows slowly in blue light and is locked in state 1. All other triple inactivation strains are constantly close to state 1
- Simultaneous inactivation of SigB and SigD (strains ΔsigBCD and ΔsigBDE) impaired acclimation to different illumination conditions and to low temperature
- ΔsigCDE has a higher carotenoid content than the control strain
- Cyanobacteria are able to grow in high iron concentrations in anaerobicity; under these conditions ferrous iron reacts with oxygen produced by photosynthesis, forming brown precipitate
- Cyanotoxins do not protect cyanobacteria from excess iron

7. ACKNOWLEDGEMENTS

This work was carried out in the Laboratory of Molecular Plant Biology at the University of Turku. Financial support from the Academy of Finland, the Finnish Cultural Foundation and the Turku University Foundation is gratefully acknowledged.

This PhD study was supervised by Esa Tyystjärvi and Taina Tyystjärvi. I am deeply grateful for your patience and guidance during this time. Professor Eevi Rintamäki and Eva-Mari Aro are thanked for providing excellent working facilities and for formal guidance of my studies. Fikret Mamedov and Eero Nikinmaa are acknowledged for critically reviewing this thesis. All my co-authors are warmly thanked.

I thank all my fellow workers and members of the technical staff. And I also wish to thank all my friends and family for their support.

Kiitos!

Turku January 2013

Susa

8. REFERENCES

Adir N (2005) Elucidation of the molecular structures of components of the phycobilisome: reconstructing a giant. Photosynth Res **85:** 15-32

Alexova R, Fujii M, Birch D, Cheng J, Waite TD, Ferrari BC, Neilan BA (2011) Iron uptake and toxin synthesis in the bloom-forming *Microcystis aeruginosa* under iron limitation. Environ Microbiol **13:** 1064-1077

Arnold W, Sherwood HK (1957) Are chloroplasts semiconductors? Proc Natl Acad Sci USA 105-114

Arteni AA, Ajlani G, Boekema EJ (2009) Structural organisation of phycobilisomes from *Synechocystis* sp. strain PCC6803 and their interaction with the membrane. BBA-Bioenergetics **1787:** 272-279

Asayama M, Imamura S (2008) Stringent promoter recognition and autoregulation by the group 3 sigma-factor SigF in the cyanobacterium *Synechocystis* sp. strain PCC 6803. Nucleic Acids Res **36:** 5297-5305

Asayama M, Imamura S, Yoshihara S, Miyazaki A, Yoshida N, Sazuka T, Kaneko T, Ohara O, Tabata S, Osanai T, Tanaka K, Takahashi H, Shirai M (2004) SigC, the group 2 sigma factor of RNA polymerase, contributes to the late-stage gene expression and nitrogen promoter recognition in the cyanobacterium *Synechocystis* sp. strain PCC 6803. Biosci Biotech Bioch **68:** 477-487

Babica P, Blaha L, Marsalek B (2006) Exploring the natural role of microcystins — A review of effects on photoautotrophic organisms. J Phycol **42:** 9-20

Bekker A, Holland H, Wang P, Rumble D, Stein H, Hannah J, Coetzee L, Beukes N (2004) Dating the rise of atmospheric oxygen. Nature **427:** 117-120

Bennett J, Steinback KE, Arntzen CJ (1980) Chloroplast phosphoproteins: regulation of excitation-energy transfer by phosphorylation of thylakoid membrane polypeptides. Proc Natl Acad Sci **77:** 5253-5257

Bhaya D, Watanabe N, Ogawa T, Grossman A (1999) The role of an alternative sigma factor in motility and pilus formation in the cyanobacterium *Synechocystis* sp. strain PCC6803. Proc Natl Acad Sci USA **96:** 3188-3193

Bibby TS, Nield J, Barber J (2001) Iron deficiency induces the formation of an antenna ring around trimeric photosystem I in cyanobacteria. Nature **412:** 743-745

Boekema E, Jensen P, Schlodder E, van Breemen J, van Roon H, Scheller H, Dekker J (2001) Green plant photosystem I binds light-harvesting complex I on one side of the complex. Biochemistry **40:** 1029-1036

Boekema E, van Breemen J, van Roon H, Dekker J (2000) Arrangement of photosystem II supercomplexes in crystalline macrodomains within the thylakoid membrane of green plant chloroplasts. J Mol Biol **301:** 1123-1133

Bonaventura C, Myers J (1969) Fluorescence and oxygen evolution from *Chlorella Pyrenoidosa*. Biochim Biophys Acta **189:** 366-383

Bontognali TRR, Sessions AL, Allwood AC, Fischer WW, Grotzinger JP, Summons RE, Eiler JM (2012) Sulfur isotopes of organic matter preserved in 3.45-billion-year-old stromatolites reveal microbial metabolism. Proc Natl Acad Sci USA **109:** 15146-15151

Boulay C, Wilson A, D'Haene S, Kirilovsky D (2010) Identification of a protein required for recovery of full antenna capacity in OCP-related photoprotective mechanism in cyanobacteria. Proc Natl Acad Sci USA **107:** 11620-11625

Bräutigam A, Weber APM (2011) Do metabolite transport processes limit photosynthesis? Plant Physiol **155:** 43-48

Brasier M, Green O, Jephcoat A, Kleppe A, Van Kranendonk M, Lindsay J, Steele A, Grassineau N (2002) Questioning the evidence for Earth's oldest fossils. Nature **416:** 76-81

Bryant DA, Frigaard N (2006) Prokaryotic photosynthesis and phototrophy illuminated. Trends Microbiol **14:** 488-496

Bryant D (2003) The beauty in small things revealed. Proc Natl Acad Sci USA **100:** 9647-9649

Cadoret JC, Demouliere R, Lavaud J, van Gorkom HJ, Houmard J, Etienne AL (2004) Dissipation of excess energy triggered by blue light in cyanobacteria with CP43' (isiA). BBA-Bioenergetics **1659:** 100-104

Cairnssmith A (1978) Precambrian solution photochemistry, inverse segregation, and banded iron formations. Nature **276:** 807-808

Callahan FE, Cheniae GM (1985) Studies on the photoactivation of the water-oxidizing enzyme: I. Processes limiting photoactivation in hydroxyl-

amine-extracted leaf segments. Plant Physiol **79:** 777-786

Chapman DJ, Vass I, Barber J (1991) Secondary-electron transfer-reactions of the isolated photosystem II reaction center after reconstitution with plastoquinone-9 and diacylglycerolipids. Biochim Biophys Acta **1057:** 391-398

Claire MW, Catling DC, Zahnle KJ (2006) Biogeochemical modelling of the rise in atmospheric oxygen. Geobiology **4:** 239-269

De Baar HJW, De Jong JTM (2001) Distriputions, sources and sinks of iron in seawater. In DR Turner, KA Hunter, eds, *Biogeochemistry of iron in seawater*. Wiley, Chichester, UK, pp 123-253

Debus RJ, Barry BA, Babcock GT, Mcintosh L (1988) Site-directed mutagenesis identifies a tyrosine radical involved in the photosynthetic oxygen-evolving system. Proc Natl Acad Sci USA **85:** 427-430

Demeter S, Vass I (1984) Charge accumulation and recombination in photosystem II studied by thermoluminescence. I. Participation of the primary acceptor Q and secondary acceptor B in the generation of thermoluminescence of chloroplasts. BBA-Bioenergetics **764:** 24-32

Demeter S, Vass I, Hideg E, sallai A (1985) Comparative thermoluminescence study of triazine-resistant and -susceptible biotypes of *Erigeron canadensis L*. BBA-Bioenergetics **806:** 16-24

Demeter S, Vass I, Horváth G, Läufer A (1984) Charge accumulation and recombination in photosystem II studied by thermoluminescence. II. Oscillation of the C band induced by flash excitation. BBA-Bioenergetics **764:** 33-39

Dittmann E, Erhard M, Kaebernick M, Scheler C, Neilan BA, von Döhren H, Börner T (2001) Altered expression of two light-dependent genes in a microcystin-lacking mutant of *Microcystis aeruginosa* PCC 7806. Microbiology **147:** 3113-3119

Dong C, Tang A, Zhao J, Mullineaux CW, Shen G, Bryant DA (2009) ApcD is necessary for efficient energy transfer from phycobilisomes to photosystem I and helps to prevent photoinhibition in the cyanobacterium *Synechococcus* sp. PCC 7002. BBA-Bioenergetics **1787:** 1122-1128

Ducruet JM, Vavilin D (1999) Chlorophyll high-temperature thermoluminescence emission as an indicator of oxidative stress: Perturbating effects of oxygen and leaf water content. Free Radical Res **31:** S187-S192

Emlyn-Jones D, Ashby MK, Mullineaux CW (1999) A gene required for the regulation of photosynthetic light harvesting in the cyanobacterium *Synechocystis* 6803. Mol Microbiol **33:** 1050-1058

Fay P (1992) Oxygen relations of nitrogen-fixation in cyanobacteria. Microbiol Rev **56:** 340-373

Ferreira KN, Iverson TM, Maghlaoui K, Barber J, Iwata S (2004) Architecture of the photosynthetic oxygen-evolving center. Science **303:** 1831-1838

Field C, Behrenfeld M, Randerson J, Falkowski P (1998) Primary production of the biosphere: Integrating terrestrial and oceanic components. Science **281:** 237-240

Ganeteg U, Kulheim C, Andersson J, Jansson S (2004) Is each light-harvesting complex protein important for plant fitness? Plant Physiol **134:** 502-509

Garlick GFJ, Gibson AF (1948) The electron trap mechanism of luminescence in sulphide and silicate phosphors. P Phys Soc **60:** 574-590

Glasstone S, Laidler KJ, Eyring H (1941) *The theory of rate processes*. McGraw-Hill, New York

Goldblatt C, Lenton TM, Watson AJ (2006) Bistability of atmospheric oxygen and the Great Oxidation. Nature **443:**

Grossman AR, Schaefer MR, Chiang GG, Collier JL (1993) The phycobilisome, a light-harvesting complex responsive to environmental-Conditions. Microbiol Rev **57:** 725-749

Gunnelius L, Tuominen I, Rantamäki S, Pollari M, Ruotsalainen V, Tyystjärvi E, Tyystjärvi T (2010) SigC sigma factor is involved in acclimation to low inorganic carbon at high temperature in *Synechocystis* sp. PCC 6803. Microbiology **156:** 220-229

Gwizdala M, Wilson A, Kirilovsky D (2011) In vitro reconstitution of the cyanobacterial photoprotective mechanism mediated by the orange carotenoid protein in *Synechocystis* PCC 6803. Plant Cell **23:** 2631-2643

Haffa ALM, Lin S, Katilius E, Williams JC, Taguchi AKW, Allen JP, Woodbury NW (2002) The dependence of the initial electron-transfer rate on driving force in *Rhodobacter sphaeroide*s reaction Centers. J Phys Chem B **106:**

Hakala M, Tuominen I, Keränen M, Tyystjärvi T, Tyystjärvi E (2005) Evidence for the role of the oxygen-evolving manganese complex in photoinhibition of photosystem II. BBA-Bioenergetics 1706:68-80

Hakala-Yatkin M, Tyystjärvi E (2011) Inhibition of photosystem II by the singlet oxygen sensor compounds TEMP and TEMPD. BBA-Bioenergetics **1807:** 243-250

Hakkila K, Antal T, Gunnelius L, Kurkela J, Matthijs HCP, Tyystjärvi E, Tyystjärvi T Group 2 sigma factor mutant ΔsigCDE reveals roles of carotenoids and flavodiiron proteins in photoprotection of photosystem II in the cyanobacterium *Synechocystis* sp. PCC 6803. Manuscript

Hideg E, Vass I (1992) The high temperature thermoluminescence band of green tissues originates in the chimiluminescence of chlorophyll promoted by free radicals. In N Murata, ed, *Research in Photosynthesis*, Vol III, Ed Murata, N. Kluwer Academic Puplishers, Netherlands, pp 107-110

Hideg E, Spetea C, Vass I (1994) Singlet oxygen and free-radical production during acceptor-induced and donor-side-induced photoinhibition: Studies with spin-trapping EPR spectroscopy. BBA-Bioenergetics **1186:** 143-152

Hihara Y, Kamei A, Kanehisa M, Kaplan A, Ikeuchi M (2001) DNA microarray analysis of cyanobacterial gene expression during acclimation to high light. Plant Cell **13:** 793-806

Huang L, McCluskey M, Ni H, LaRossa R (2002) Global gene expression profiles of the cyanobacterium *Synechocystis* sp. strain PCC 6803 in response to irradiation with UV-B and white light. J Bacteriol **184:** 6845-6858

Humble A, Gadd G, Codd G (1997) Binding of copper and zinc to three cyanobacterial microcystins quantified by differential pulse polarography. Water Res **31:** 1679-1686

Imamura S, Asayama M, Takahashi H, Tanaka K, Takahashi H, Shirai M (2003) Antagonistic dark/light-induced SigB/SigD, group 2 sigma factors, expression through redox potential and their roles in cyanobacteria. FEBS Lett **554:** 357-362

Imamura S, Tanaka K, Shirai M, Asayama M (2006) Growth phase-dependent activation of nitrogen-related genes by a control network of group 1 and group 2 sigma factors in a cyanobacterium. J Biol Chem **281:** 2668-2675

Imamura S, Yoshihara S, Nakano S, Shiozaki N, Yamada A, Tanaka K, Takahashi H, Asayama M, Shirai M (2003) Purification, characterization, and gene expression of all sigma factors of RNA polymerase in a cyanobacterium. J Mol Biol **325:** 857-872

Inoue Y (1981) Charging of the a band of thermoluminescence, dependent on the S_3 state in isolated chloroplasts. BBA-Bioenergetics **634:** 309-320

Isley A, Abbott D (1999) Plume-related mafic volcanism and the deposition of banded iron formation. J Geophys Res-Sol Ea **104:** 15461-15477

Ivanov AG, Krol M, Sveshnikov D, Selstam E, Sandstrom S, Koochek M, Park Y, Vasil'ev S, Bruce D, Oquist G, Huner NPA (2006) Iron deficiency in cyanobacteria causes monomerization of photosystem I trimers and reduces the capacity for state transitions and the effective absorption cross section of photosystem I in vivo. Plant Physiol **141:** 1436-1445

Jaiswal P, Singh PK, Prasanna R (2008) Cyanobacterial bioactive molecules — an overview of their toxic properties. Can J Microbiol **54:** 701-717

James H, L. (1954) Sedimentary facies of iron-formation. Econ Geol **49:** 235-293

Jansson S (1994) The light-harvesting chlorophyll *a*/*b* binding-proteins. BBA-Bioenergetics **1184:** 1-19

JegerschÖld C, Styring S (1996) Spectroscopic characterization of intermediate steps involved in donor-side-induced photoinhibition of photosystem II. Biochemistry **35:** 7794-7801

Joliot A, Joliot P (1964) Etude cinetique de la reaction photochimique liberant loxygene au cours de la photosynthese. C R Acad Sci **258:** 4622-4625

Jordan P, Fromme P, Witt H, Klukas O, Saenger W, Krauss N (2001) Three-dimensional structure of cyanobacterial photosystem I at 2.5 angstrom resolution. Nature **411:** 909-917

Kaneko T, Tanaka A, Sato S, Kotani H, Sazuka T, Miyajima N, Sugiura M, Tabata S (1995) Sequence analysis of the genome of the unicellular cyanobacterium *Synechocystis* sp. strain PCC6803. I. Sequence features in the 1 Mb region from map positions 64% to 92% of the genome. DNA Res **2:** 153-166

Kanesaki Y, Yamamoto H, Paithoonrangsarid K, Shoumskaya M, Suzuki I, Hayashi H, Murata N (2007) Histidine kinases play important roles in the perception and signal transduction of hydrogen peroxide in the cyanobacterium, *Synechocystis* sp. PCC 6803. Plant J **49:** 313-324

Keeling P (2004) Diversity and evolutionary history of plastids and their hosts. Am J Bot **91:** 1481-1493

Keränen M, Aro E, Nevalainen O, Tyystjärvi E (2009) Toxic and non-toxic *Nodularia* strains can be distinguished from each other and from eukaryotic algae with chlorophyll fluorescence fingerprinting. Harmful Algae **8:** 817-822

Keren N, Gong HS, Ohad I (1995) Oscillations of reaction-center-II D1-protein-degradation in-vivo induced by repetitive light-flashes. Correlation between the level of RCII-Q_B^-, and protein-degradation in low-light. J Biol Chem **270:** 806-814

Kirchhoff H, Borinski M, Lenhert S, Chi L, Buchel C (2004) Transversal and lateral exciton energy transfer in grana thylakoids of spinach. Biochemistry **43:** 14508-14516

Koike H, Siderer Y, Ono T-, Inoue Y (1986) Assignment of thermoluminescence A band to $S_3Q_A^-$ charge recombination: Sequential stabilization of S_3 and Q_A^- by a two-step illumination at different temperatures. BBA-Bioenergetics **850:** 80-89

Kok B, Forbush B, Mcgloin M (1970) Cooperation of charges in photosynthetic O_2 evolution-I. A linear four step mechanism. Photochem Photobiol **11:** 457-475

Konhauser KO, Hamade T, Raiswell R, Morris RC, Ferris FG, Southam G, Canfield DE (2002) Could bacteria have formed the Precambrian banded iron formations? Geology **30:** 1079-1082

Kouril R, Arteni A, Lax J, Yeremenko N, D'Haene S, Rogner M, Matthijs H, Dekker J, Boekema E (2005) Structure and functional role of supercomplexes of IsiA and photosystem I in cyanobacterial photosynthesis. FEBS Lett **579:** 3253-3257

Kucho K, Okamoto K, Tsuchiya Y, Nomura S, Nango M, Kanehisa M, Ishiura M (2005) Global analysis of circadian expression in the cyanobacterium *Synechocystis* sp. strain PCC 6803. J Bacteriol **187:** 2190-2199

Lavergne J, Trissl HW (1995) Theory of fluorescence induction in photosystem-II: Derivation of analytical expressions in a model including exciton-radical-pair equilibrium and restricted energy-transfer between photosynthetic units. Biophys J **68:** 2474-2492

Lavorel J (1975) Luminescence. In: Govindjee (ed) *Bioenergetics of photosynthesis*. Academic Press, New York, pp. 223-317

Lemeille S, Rochaix J (2010) State transitions at the crossroad of thylakoid signalling pathways. Photosynth Res **106:** 33-46

Li XP, Björkman O, Shih C, Grossman AR, Rosenquist M, Jansson S, Niyogi KK (2000) A pigment-binding protein essential for regulation of photosynthetic light harvesting. Nature **403:** 391-395

Lonetto M, Gribskov M, Gross CA (1992) The σ^{70} family: Sequence conservation and evolutionary relationships. J Bacteriol **174:** 3843-3849

Loukos H, Frost B, Harrison D, Murray J (1997) An ecosystem model with iron limitation of primary production in the equatorial Pacific at 140 degrees W. Deep-Sea Res Pt II **44:** 2221-2249

Lukac M, Aegerter R (1993) Influence of trace-metals on growth and toxin production of *Microcystis-Aeruginosa*. Toxicon **31:** 293-305

MacColl R (1998) Cyanobacterial phycobilisomes. J Struct Biol **124:** 311-334

Marcus R, Sutin N (1985) Electron transfer in chemistry and biology. Biochim Biophys Acta **811:** 265-322

Marin K, Suzuki L, Yamaguchi K, Ribbeck K, Yamamoto H, Kanesaki Y, Hagemann M, Murata N (2003) Identification of histidine kinases that act as sensors in the perception of salt stress in *Synechocystis* sp. PCC 6803. Proc Natl Acad Sci USA **100:** 9061-9066

Martin J (1990) Glacial-interglacial CO_2 change: The iron hypothesis. Paleoceanography **5:** 1-13

Matsui M, Yoshimura T, Wakabayashi Y, Imamura S, Tanaka K, Takahashi H, Asayama M, Shirai M (2007) Interference expression at levels of the transcript and protein among group 1, 2, and 3 sigma factor genes in a cyanobacterium. Microbes Environ **22:** 32-43

Meriluoto J, Codd GA, (2005) *TOXIC: Cyanobacterial monitoring and cyanotoxin Analysis.* Åbo Akademi university press, Turku

Misra H, Tuli R (2000) Differential expression of photosynthesis and nitrogen fixation genes in the cyanobacterium *Plectonema boryanum*. Plant Physiol **122:** 731-736

Moser CC, Page CC, Dutton PL (2006) Darwin at the molecular scale: selection and variance in electron tunnelling proteins including cytochrome *c* oxidase. Philos T Roy Soc B **361:**

Mullineaux CW (2008) Phycobilisome-reaction centre interaction in cyanobacteria. Photosynth Res **95:** 175-182

Mullineaux CW (1992) Excitation-energy transfer from phycobilisomes to photosystem I in a cyanobacterium. Biochim Biophys Acta **1100:** 285-292

Mullineaux C, Tobin M, Jones G (1997) Mobility of photosynthetic complexes in thylakoid membranes. Nature **390:** 421-424

Murata N (1969) Control of excitation transfer in photosynthesis I. Light-induced change of chlorophyll *a* fluorescence in *Porphyridium Cruentum*. Biochim Biophys Acta **172:** 242-251

Muro-Pastor AM, Herrero A, Flores E (2001) Nitrogen-regulated group 2 sigma factor from *Synechocystis* sp. strain PCC 6803 involved in survival under nitrogen stress. J Bacteriol **183:** 1090-1095

Nikkinen H, Hakkila K, Gunnelius L, Huokko T, Pollari M, Tyystjärvi T (2012) The SigB sigma factor regulates multiple salt acclimation responses of the cyanobacterium *Synechocystis* sp. PCC 6803. Plant Physiol **158:** 514-523

Nisbet E, Sleep N (2001) The habitat and nature of early life. Nature **409:** 1083-1091

Niyogi KK, Li XP, Rosenberg V, Jung HS (2005) Is PsbS the site of non-photochemical quenching in photosynthesis? J Exp Bot **56:** 375-382

Noguchi T, Inoue Y, Sonoike K (1993) Thermoluminescence emission at liquid-helium temperatures from photosynthetic apparatus and purified pigments. Biochim Biophys Acta **1141:** 18-22

Ohmoto H, Watanabe Y, Ikemi H, Poulson SR, Taylor BE (2006) Sulphur isotope evidence for an oxic Archaean atmosphere. Nature **442:**

Osanai T, Azuma M, Tanaka K (2007) Sugar catabolism regulated by light- and nitrogen-status in the cyanobacterium *Synechocystis* sp. PCC 6803. Photochem Photobiol Sci **6:** 508-514

Osanai T, Imashimizu M, Seki A, Sato S, Tabata S, Imamura S, Asayama M, Ikeuchi M, Tanaka K (2009) ChlH, the H subunit of the Mg-chelatase, is an anti-sigma factor for SigE in *Synechocystis* sp. PCC 6803. Proc Natl Acad Sci USA **106:** 6860-6865

Osanai T, Kanesaki Y, Nakano T, Takahashi H, Asayama M, Shirai M, Kanehisa M, Suzuki I, Murata N, Tanaka K (2005) Positive regulation of sugar catabolic pathways in the cyanobacterium *Synechocystis* sp. PCC 6803 by the group 2 sigma factor *sigE*. J Biol Chem **280:** 30653-30659

Paithoonrangsarid K, Shoumskaya M, Kanesaki Y, Satoh S, Tabata S, Los D, Zinchenko V, Hayashi H, Tanticharoen M, Suzuki I, Murata N (2004) Five histidine kinases perceive osmotic stress and regulate distinct sets of genes in *Synechocystis*. J Biol Chem **279:** 53078-53086

Parekh P, Follows M, Boyle E (2004) Modeling the global ocean iron cycle. Global Biogeochem Cy **18:** GB1002

Pierson BK (1994) The emergence, diversification, and role of photosynthetic eubacteria. In Y Cohen, E Rosenberg, eds, *Microbial Mat: Physiological Ecology of Benthic Microbial Communities*. Am. Soc. Microbiol., Washinton, DC, pp 402-427

Pollari M, Gunnelius L, Tuominen I, Ruotsalainen V, Tyystjärvi E, Salminen T, Tyystjärvi T (2008) Characterization of single and double inactivation strains reveals new physiological roles for group 2 sigma factors in the cyanobacterium *Synechocystis* sp. PCC 6803. Plant Physiol **147:** 1994-2005

Pollari M, Ruotsalainen V, Rantamäki S, Tyystjärvi E, Tyystjärvi T (2009) Simultaneous inactivation of sigma factors B and D interferes with light acclimation of the cyanobacterium *Synechocystis* sp. Strain PCC 6803. J Bacteriol **191:** 3992-4001

Punginelli C, Wilson A, Routaboul J, Kirilovsky D (2009) Influence of zeaxanthin and echinenone binding on the activity of the orange carotenoid protein. BBA-Bioenergetics **1787:** 280-288

Randall JT, Wilkins MHF (1945) Phosphorescence and electron traps .I. The study of trap distributions. Proc Roy Soc Lond A Mat **184:** 336-389

Rantala A, Fewer D, Hisbergues M, Rouhiainen L, Vaitomaa J, Borner T, Sivonen K (2004) Phylogenetic evidence for the early evolution of microcystin synthesis. Proc Natl Acad Sci USA **101:** 568-573

Rappaport F, Cuni A, Xiong L, Sayre R, Lavergne R (2005) Charge recombination and thermoluminescence in photosystem II. Biophys J **88:** 1948-1958

Rappaport F, Guergova-Kuras M, Nixon P, Diner B, Lavergne J (2002) Kinetics and pathways of charge recombination in photosystem II. Biochemistry **41:** 8518-8527

Rappaport F, Lavergne J (2009) Thermoluminescence: theory. Photosynth Res **101:** 205-216

Renger G, Hanssum B (2009) Oxygen detection in biological systems. Photosynth Res **102:** 487-498

Rodriguez-Ezpeleta N, Brinkmann H, Burey S, Roure B, Burger G, Loffelhardt W, Bohnert H, Philippe H, Lang B (2005) Monophyly of primary photosynthetic eukaryotes: Green plants, red algae, and glaucophytes. Curr Biol **15:** 1325-1330

Rosing M, Rose N, Bridgwater D, Thomsen H (1996) Earliest part of Earth's stratigraphic record: A reappraisal of the >3.7 Ga Isua (Greenland) supracrustal sequence. Geology **24:** 43-46

Rutherford AW, Crofts AR, Inoue Y (1982) Thermoluminescence as a probe of photosystem II photochemistry. The origin of the flash-induced glow peaks. BBA- Bioenergetics **682:** 457-465

Rutherford AW, Inoue Y (1984) Oscillation of delayed luminescence from PS-II: recombination of $S_2Q_B^-$ and $S_3Q_B^-$. FEBS Lett **165:** 163-170

Sarcina M, Tobin MJ, Mullineaux CW (2001) Diffusion of phycobilisomes on the thylakoid membranes of the cyanobacterium *Synechococcus* 7942. Effects of phycobilisome size, temperature, and membrane lipid composition. J Biol Chem **276:** 46830-46834

Schidlowski M (1988) A 3,800-million-year isotopic record of life from carbon in sedimentary-rocks. Nature **333:** 313-318

Schneider GJ, Tumer NE, Richaud C, Borbely G, Haselkorn R (1987) Purification and characterization of RNA-polymerase from the cyanobacterium *Anabaena* 7120. J Biol Chem **262:** 14633-14639

Schneider G, Haselkorn R (1988) RNA-polymerase subunit homology among cyanobacteria, other eubacteria, and archaebacteria. J Bacteriol **170:** 4136-4140

Schopf J (1993) Microfossils of the early archean apex chert: New evidence of the antiquity of life. Science **260:** 640-646

Schopf J, Packer B (1987) Early archean (3.3-Billion to 3.5-Billion-Year-Old) microfossils from Warrawoona Group, Australia. Science **237:** 70-73

Seki A, Hanaoka M, Akimoto Y, Masuda S, Iwasaki H, Tanaka K (2007) Induction of a group 2 sigma factor, RPOD3, by high light and the underlying mechanism in *Synechococcus elongatus* PCC 7942. J Biol Chem **282:** 36887-36894

Sonoike K, Koike H, Enami I, Inoue Y (1991) The emission-spectra of thermoluminescence from the photosynthetic apparatus. Biochim Biophys Acta **1058:** 121-130

Strasser R, Stirbet A (2001) Estimation of the energetic connectivity of PSII centres in plants using the fluorescence rise O-J-I-P. Fitting of experimental data to three different PSII models. Math Comput Simulat **56:** 451-461

Strehler BL, Arnold W (1951) Light production by green plants. J Gen Physiol **34:** 809-820

Summerfield TC, Sherman LA (2007) Role of sigma factors in controlling global gene expression in light/dark transitions in the cyanobacterium *Synechocystis* sp. strain PCC 6803. J Bacteriol **189:** 7829-7840

Summons R, Jahnke L, Hope J, Logan G (1999) 2-Methylhopanoids as biomarkers for cyanobacterial oxygenic photosynthesis. Nature **400:** 554-557

Tian L, Gwizdala M, van Stokkum IHM, Koehorst RBM, Kirilovsky D, van Amerongen H (2012) Picosecond kinetics of light harvesting and photoprotective quenching in wild-type and mutant phycobilisomes isolated from the cyanobacterium *Synechocystis* PCC 6803. Biophys J **102:** 1692-1700

Tuominen I, Pollari M, Tyystjärvi E, Tyystjärvi T (2006) The SigB sigma factor mediates high-temperature responses in the cyanobacterium *Synechocystis* sp. PCC6803. FEBS Lett **580:** 319-323

Tuominen I, Pollari M, Von Wobeser EA, Tyystjärvi E, Ibelings BW, Matthijs HCP, Tyystjärvi T (2008) Sigma factor SigC is required for heat acclimation of the cyanobacterium *Synechocystis* sp. strain PCC 6803. FEBS Lett **582:** 346-350

Tuominen I, Tyystjärvi E, Tyystjärvi T (2003) Expression of primary sigma factor (PSF) and PSF-like sigma factors in the cyanobacterium *Synechocystis* sp. strain PCC 6803. J Bacteriol **185:** 1116-1119

Tyystjärvi E, Vass I (2004) Light emission as a probe of charge separation and recombination in the photosynthetic apparatus: Relation of prompt fluorescence to delayed light emission and thermoluminescence. In GC Papageorgiou, Govindjee, eds, *Chlorophyll fluorescence: A signature of photosynthesis.* Kluwer Academic Publishers, The Netherlands, pp 363-388

Umena Y, Kawakami K, Shen J, Kamiya N (2011) Crystal structure of oxygen-evolving photosystem II at a resolution of 1.9 angstrom. Nature **473:** 55-U65

Utkilen H, Gjolme N (1995) Iron-Stimulated toxin production in *Microcystis-Aeruginosa*. Appl Environ Microb **61:** 797-800

van Thor J, Mullineaux C, Matthijs H, Hellingwert K (1998) Light harvesting and state transitions in cyanobacteria. Bot Acta **111:** 430-443

Vass I, Chapmann D, Barber J (1989) Thermoluminescence properties of the isolated photosystem two reaction center. Photosynth Res **22:** 295-301

Vass I, Horvath G, Herczeg T, Demeter S (1981) Photosynthetic energy-conservation investigated by thermo-luminescence - activation-energies and half-lives of thermo-luminescence bands of chloroplasts determined by mathematical resolution of glow curves. Biochim Biophys Acta **634:** 140-152

Vass I, Styring S, Hundal T, Koivuniemi A, Aro E, Andersson B (1992) Reversible and irreversible intermediates during photoinhibition of photosystem II: Stable reduced Q_A species promote chlorophyll triplet formation. Proc Natl Acad Sci USA **89:** 1408-1412

Vogel AI (1962) *A text-book of quantative inorganic analysis*. Wiley, New York

Wang XJ, Behrenfeld M, Le Borgne R, Murtugudde R, Boss E (2009) Regulation of phytoplankton carbon to chlorophyll ratio by light, nutrients and temperature in the Equatorial Pacific Ocean: a basin-scale model. Biogeosciences **6:** 391-404

Widdel F, Schnell S, Heising S, Ehrenreich A, Assmus B, Schink B (1993) Ferrous iron oxidation by anoxygenic phototrophic bacteria. Nature **362:** 834-836

Wientjes E, van Stokkum IHM, van Amerongen H, Croce R (2011) The role of the individual Lhcas in photosystem I excitation energy trapping. Biophys J **101:** 745-754

Williams JGK (1988) Construction of specific mutations in photosystem-II photosynthetic reaction center by genetic-engineering methods in *Synechocystis*-6803. Methods Enzymol **167:** 766-778

Wilson A, Ajlani G, Verbavatz JM, Vass I, Kerfeld CA, Kirilovsky D (2006) A soluble carotenoid protein involved in phycobilisome-related energy dissipation in cyanobacteria. Plant Cell **18:** 992-1007

Wilson A, Boulay C, Wilde A, Kerfeld CA, Kirilovsky D (2007) Light-induced energy dissipation in iron-starved cyanobacteria: roles of OCP and IsiA proteins. Plant Cell **19:** 656-672

Wilson A, Kinney JN, Zwart PH, Punginelli C, D'Haene S, Perreau F, Klein MG, Kirilovsky D, Kerfeld CA (2010) Structural determinants underlying photoprotection in the photoactive orange carotenoid protein of cyanobacteria. J Biol Chem **285:** 18364-18375

Wilson A, Punginelli C, Gall A, Bonetti C, Alexandre M, Routaboul J, Kerfeld CA, van Grondelle R, Robert B, Kirilovsky D (2008) A photoactive carotenoid protein acting as light intensity sensor. Proc Natl Acad Sci USA **105:** 12075-12080

Zhang P, Allahverdiyeva Y, Eisenhut M, Aro E (2009) Flavodiiron proteins in oxygenic photosynthetic organisms: photoprotection of photosystem II by Flv2 and Flv4 in *Synechocystis* sp. PCC 6803. Plos One **4:** e5331

Zhang P, Eisenhut M, Brandt A, Carmel D, Silen HM, Vass I, Allahverdiyeva Y, Salminen TA, Aro E (2012) Operon *flv4-flv2* provides cyanobacterial photosystem II with flexibility of electron transfer. Plant Cell **24:** 1952-1971

Zubkov M, Sleigh M, Burkill P, Leakey R (2000) Picoplankton community structure on the Atlantic Meridional Transect: a comparison between seasons. Prog Oceanogr **45:** 369-386